


Review

Two-Dimensional Layered Double Hydroxides for Reactions of Methanation and Methane Reforming in C1 Chemistry

Panpan Li ¹, Feng Yu ^{1,*} , Naveed Altaf ², Mingyuan Zhu ¹, Jiangbing Li ¹, Bin Dai ¹ and Qiang Wang ^{1,2,*}

¹ Key Laboratory for Green Processing of Chemical Engineering of Xinjiang Bingtuan, School of Chemistry and Chemical Engineering, Shihezi University, Shihezi 832003, China; ppl_19910109@163.com (P.L.); zhumin yuan@shzu.edu.cn (M.Z.); ljbin@shzu.edu.cn (J.L.); db_tea@shzu.edu.cn (B.D.)

² Environmental Functional Nanomaterials (EFN) Laboratory, College of Environmental Science and Engineering, Beijing Forestry University, Beijing 100083, China; naveed007@bjfu.edu.cn

* Correspondence: yufeng05@mail.ipc.ac.cn (F.Y.); qiangwang@bjfu.edu.cn (Q.W.); Tel.: +86-993-205-7272 (F.Y.); Fax: +86-993-205-7270 (F.Y.)

Received: 27 December 2017; Accepted: 28 January 2018; Published: 31 January 2018

Abstract: CH₄ as the paramount ingredient of natural gas plays an eminent role in C1 chemistry. CH₄ catalytically converted to syngas is a significant route to transmute methane into high value-added chemicals. Moreover, the CO/CO₂ methanation reaction is one of the potent technologies for CO₂ valorization and the coal-derived natural gas production process. Due to the high thermal stability and high extent of dispersion of metallic particles, two-dimensional mixed metal oxides through calcined layered double hydroxides (LDHs) precursors are considered as the suitable supports or catalysts for both the reaction of methanation and methane reforming. The LDHs displayed compositional flexibility, small crystal sizes, high surface area and excellent basic properties. In this paper, we review previous works of LDHs applied in the reaction of both methanation and methane reforming, focus on the LDH-derived catalysts, which exhibit better catalytic performance and thermal stability than conventional catalysts prepared by impregnation method and also discuss the anti-coke ability and anti-sintering ability of LDH-derived catalysts. We believe that LDH-derived catalysts are promising materials in the heterogeneous catalytic field and provide new insight for the design of advance LDH-derived catalysts worthy of future research.

Keywords: layered double hydroxides; two-dimensional materials; methanation reaction; methane reforming; C1 chemistry

1. Introduction

CH₄ as a valuable ingredient of natural gas, biogas and coal mine gas plays a prestigious role in C1 chemistry. CH₄ utilization is an important method to utilize greenhouse gas to protect resources and the environment, and methane catalytically-converted into syngas is a preeminent route to synthesize high added-value chemicals from methane [1,2]. The routes for converting methane to syngas include dry reforming of methane (DRM), steam reforming of methane (SRM), partial oxidation of methane (POM) and autothermal reforming (ATM) [3–8]. Among the four kinds of routes for converting methane to syngas, SMR is the most common and renowned economic way to utilize CH₄ and produce H₂ and have been applied at the industry scale [9]. Besides, POM can obtain a suitable CO/H₂ ratio for methanol synthesis and possesses the advantages of high energy efficiency and mild exothermicity, which exhibit great potential in small reactors that are ideal for decentralized applications [10–12]. When combining SMR and POM, namely autothermal reforming (ATR), exothermic methane oxidation

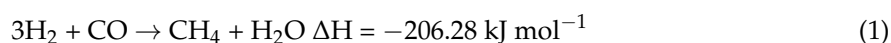
can provide energy to endothermic steam reforming, thus a large external supply of heat can be avoided. ATR possesses the superiority of easy reactor temperature control and avoids catalyst sintering and carbon deposition, and a wider range of H₂/CO ratio can be obtained by manipulating the relative concentrations of H₂O and O₂, as well [13–15]. Furthermore, CH₄ can also be obtained by CO/CO₂ methanation, which is a tremendously effectual technology for CO₂ valorization and processes for coal-derived natural gas production. CO methanation is an effective way to produce CH₄, and the clean utilization of coal in regions abundant in coal and lacking natural gas has been realized [16,17]. Additionally, CO₂ methanation plays an important role in the “power to gas” process and also is an efficient method to produce CH₄ and mitigate CO₂ emissions, which comprise one of the main sources of global warming [18–23]. Layered double hydroxides (LDHs) have a general molecular formula of [M(II)_(1-x)M(III)_x(OH)₂]^{x+}[A_{x/n}ⁿ⁻]_n·mH₂O, where M(II) represents divalent cations (e.g., Mg, Ni, etc.), M(III) is trivalent cations (e.g., Al, Fe, etc.) and Aⁿ⁻ denotes anions [24]. LDHs possess compositional flexibility due to the changeable composition and possess a “memory effect” [25–30]. The “memory effect”, i.e., after mild thermal treatment, of LDHs can be reconstructed when contacting the solutions containing various anions [31]. LDH-derived catalysts can form homogeneous mixtures of oxides with a small crystal size, which are stable to thermal treatments and eventually exhibit high thermal stability during high temperature reactions [32]. Due to the high thermal stability and high extent of dispersion of metallic particles, redox stability and Lewis acidity, LDH precursor-derived mixed metal oxides are considered also as qualified supports or catalysts for heterogeneous catalysis.

The active components of catalysts for methanation and methane reforming are similar or equivalent, and the similar reactions are highly exothermic, so conventional supported catalysts easily sinter at high temperatures, leading to catalytic deactivation [33]. The active component can be supported on the surface of LDHs or act as a component of LDHs and form a periclase-like structure to restrain the active component Ni’s agglomeration [34]. LDH-derived catalysts exhibit good thermo-stability and have been widely studied in CO/CO₂ methanation and methane reforming, which exhibit excellent catalytic performance, as well as anti-coke and anti-sintering abilities. In this paper, a critical review of LDH-derived catalysts for both methanation and methane reforming has been carried out. The catalytic performance, thermal stability, anti-coke and anti-sintering abilities of such catalysts will be discussed assiduously. We believe that the LDH-derived catalysts are promising for the methanation and methane reforming in C1 chemistry.

2. Methanation

2.1. CO Methanation

The methanation reaction is an ideal way for the coal-derived natural gas production process, for which the catalyst is the key. The reaction of CO methanation is described in Equation (1) [35].



Ni-based catalysts are the most suitable catalysts when taking catalytic performance and cost into consideration [36]. Metallic oxides (Al₂O₃, MgO, TiO₂, ZrO₂, CeO₂, etc.) and molecular sieves (MCM-41, SBA-15, etc.) have been employed to act as support for CO methanation catalysts and exhibit good catalytic performance [37–39]. However, many traditional supported Ni-based catalysts always possess poor dispersion of the active component and deactivation at high temperatures due to coke formation and active component sintering [40,41]. LDH-derived catalysts show high surface area, uniform metal dispersion and a good thermal property and have been used as catalysts for oxidation of methane, hydrogen production from ethanol and CO methanation, as summarized in Figure 1 [42].

Ni-Al LDH-derived catalysts have been deeply investigated and are well known for CO methanation. In 1994, Rathouskf et al. [43] formulated NiAl-CO₃ LDH-derived mixed oxide (NiAl-LDO) as the CO methanation catalyst, which maintained excellent activity for the methanation reaction under 2 MPa and 527 °C. The NiAl-LDO catalyst with 56.5 wt % Ni achieved 97% of CO conversion in the

pilot methanation unit. Except for the co-precipitation method, the urea hydrolysis method is also an effective route for preparing Ni/Al LDH. Meanwhile, Bian et al. [35] synthesized Ni/Al LDH through the urea hydrolysis method, and the resulting NiAl-LDO catalyst displayed higher catalytic stability due to higher Ni dispersion and stronger resistance to coke deposition compared with the impregnated catalyst. Nearly 100% CO conversion was achieved under reaction temperatures between 400 and 500 °C with a gaseous hourly space velocity (GHSV) of 300,000 mL g⁻¹ h⁻¹.

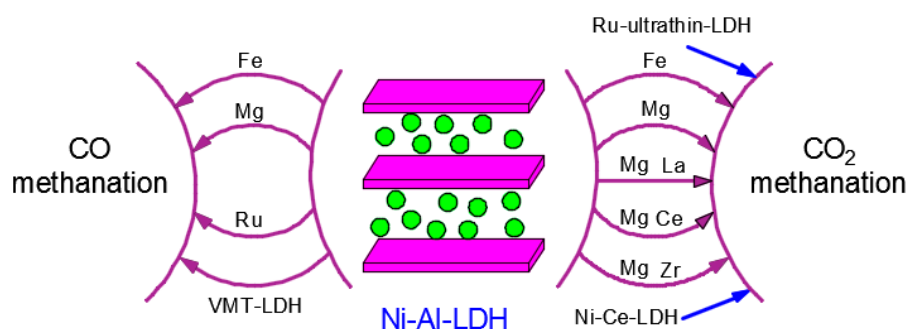


Figure 1. The applications of layered double hydroxides (LDHs) in CO and CO₂ methanation.

However, in the methanation reaction, Ni/Al LDHs also have some drawbacks; for instance, the high nickel content could lead to nickel sintering and carbon deposition during long-term operation [44,45]. Promoters can be released as a drawback, and Hwang et al. [46] reported that the performance of mesoporous nickel-M-alumina xerogel catalysts can be enhanced by introducing a promoter. They found that the yield for CH₄ decreased in the order of 30Ni10FeAX > 30Ni10NiAX > 30Ni10CoAX > 30Ni10CeAX > 30Ni10LaAX. The 30Ni10FeAX catalyst exhibited the optimal CO dissociation energy and largest H₂ adsorption ability, which played a key role in determining the catalytic performance, and thus, Fe was regarded as the most suitable second metal component. The 30Ni10FeAX catalyst achieved 99.4% CO conversion and 79.1% CH₄ yield at 230 °C. Kustov et al. [47] evaluated the influence of the Ni/Fe ratio and the total metal loading on catalytic performance. Two series of mono- and bi-metallic Ni-Fe catalysts were prepared and the catalytic properties tested, among which 25Fe75Ni catalysts were the most active in CO hydrogenation for the MgAl₂O₄ support at low metal loadings. The maximum performance of 25Fe75Ni catalysis could be obtained at 20 wt % total metal loading, exhibiting 100% CO conversion and 99.1% CH₄ selectivity at 275 °C under a GHSV = 50,000 h⁻¹.

Besides, Mg adulteration can improve the anti-coke ability of Ni/Al LDHs. Li et al. [48] synthesized Ni/Mg/Al LDHs through the co-precipitation method, and the as-obtained NiMg8 (Ni/Mg = 1/8) catalyst with 11 wt % Ni content achieved the best CO methanation performance due to the small size of Ni particles, a higher extent of Ni dispersion and the strong interaction between Ni and MgO and/or Al₂O₃ leads to form Ni_xMg_{1-x}O solid solution during calcination treatment of the Ni/Mg/Al LDH precursor; both properties benefited NiMg8 catalyst, exhibiting an excellent performance. NiMg8 catalyst achieved 99.8% CO conversion and 73.6% CH₄ selectivity at 550 °C. In our previous work, we have the spent liquor after mixed-acid etching of vermiculite (VMT) (Figure 2), which mainly contained Mg²⁺ and Al³⁺, to synthesize a VMT-derived LDH (VMT-LDH) and prepared Ni/VMT-LDO through the impregnation method. Due to Fe and Ca modification and the improved dispersion of nickel, Ni/VMT-LDO catalyst had smaller Ni nanoparticles than Ni/MgAl-LDO catalyst, leading to better performance than Ni/MgAl-LDO. Compared with Ni/MgAl-LDO, Ni/VMT-LDO catalyst showed good low temperature activity and achieved 87.9% CO conversion, as well as 90% CH₄ selectivity at 400 °C [34].

In addition, noble metal doping can not only enhance the NiO reducibility to generate active sites, but also can act as an active component itself, which was favorable for CO methanation. Concurrently, Mohaideen et al. [42] added 1 wt % Ru to NiAl-mixed metal oxides, and the as-obtained catalyst has

small Ru particles, which modified the interaction between Ru and Ni, increased the reducibility of NiO and generated more active sites for the CO methanation reaction. Subsequently, Ru/NiAl-C catalysts achieved a CO conversion of almost 100% in the temperature range from 150–220 °C. Catalytic performance of CO methanation for different catalysts in different works were summarized in Table 1.

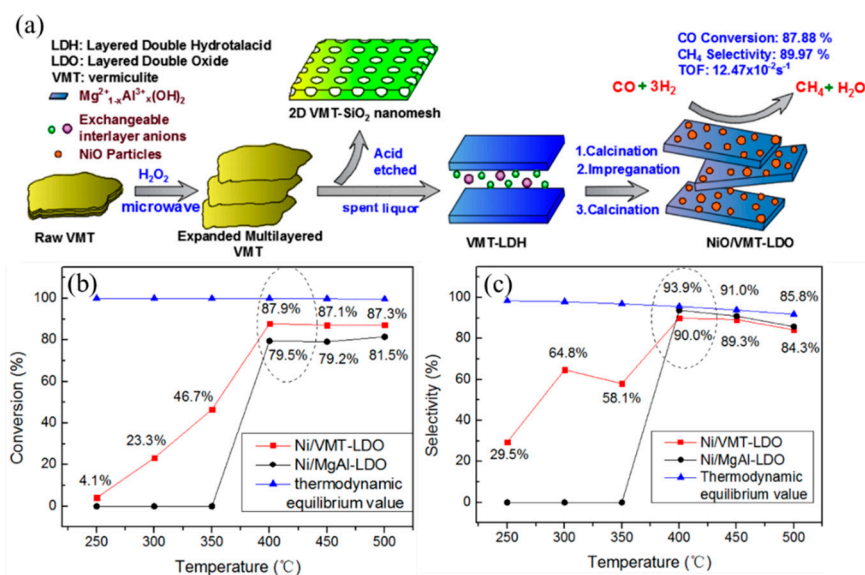


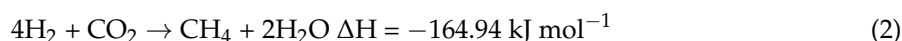
Figure 2. (a) Schematic of the preparation process of NiO/VMT-LDO and (b,c) the catalytic performance of Ni/VMT-LDO [34].

Table 1. Catalytic performance of CO methanation for different catalysts in different works.

Catalyst	Ni (wt %)	Temperature (°C)	Pressure (MPa)	GHSV (mL g ⁻¹ h ⁻¹)	CO Conversion (%)	CH ₄ Selectivity (%)	Ref.
NiMg8	11	550	0.1	15,000 h ⁻¹	99.8	73.6	[48]
Ru/NiAl-C	30	150	0.1	2400 h ⁻¹	100	–	[42]
NiAl-LDO	50 mol %	400	0.1	300,000	100	90	[35]
Ni/VMT-LDO	10	400	1.5	20,000	87.9	90	[34]
30Ni10FeAX	30	230	1	8160	99.4	79.6	[46]
25Fe75Ni	5	275	–	50,000 h ⁻¹	100	99.1	[42]

2.2. CO₂ Methanation

CO₂ methanation is one of the most eloquent technologies for CO₂ valorization and played an important role in the “power to gas” process [48]. The equation of CO methanation is as follows [35,49]:



The active components and supports of catalysts for CO methanation and CO₂ methanation are similar or equivalent; similar to CO methanation, metallic oxides (Al₂O₃, MgO, TiO₂, ZrO₂, CeO₂, etc.) are used as catalysts [21,50–54]. However, similar to the CO methanation catalyst, the main concern is catalyst sintering and carbon deposition, and LDH-derived Ni catalysts present good resistance to coking and sintering under methanation of CO at high temperatures; LDH-derived catalysts are also potential catalysts for CO₂ methanation.

Similar to CO methanation, Ni-Al LDH was also a commonly-used catalyst. Abate et al. [50] synthesized Ni-Al LDH through the co-precipitation method for CO₂ methanation. The as-obtained catalyst exhibited better performance compared with commercial catalysts due to the higher metal surface area and metal dispersion. Ni-Al12 catalyst, which was prepared at a pH of 12, has achieved

86% CO₂ conversion at 300 °C, with a GHSV of 5000 h⁻¹. Gabrovska et al. [51] revealed that the sample with Ni/Al = 3 exhibited the highest conversion during all the reactions after reduction at 400 and 450 °C, while the catalyst of Ni/Al = 0.5 surpassed the catalytic performance of Ni/Al = 3 after reduction within 530–600 °C due to the increase of Ni⁰ dispersion.

The precipitation rate and agglomerates varied with hydrophilic colloids, which resulted in diverse metal particle size and further influenced the catalytic performance. The precipitation rate of NaOH, NH₄OH, Na₂CO₃ and (NH₄)₂CO₃ was different; precipitation rate of hydrophilic colloids in Na⁺-based liquors was faster than that in NH₄⁺-based liquors; and the metal particle size of the as-obtained catalysts decreased in the order of NiFeAl-NaOH > NiFeAl-NH₄OH > NiFeAl-Na₂CO₃ > NiFeAl-(NH₄)₂CO₃. The increasing order of different catalysts performance is NiFeAl-NaOH < NiFeAl-NH₄OH < NiFeAl-Na₂CO₃ < NiFeAl-(NH₄)₂CO₃ [55]. (Ni,Mg,Al)-LDH-derived catalyst was first used as a CO₂ methanation catalyst by Bette et al. [56]. The as-prepared catalyst reached a maximum of (74 ± 2)% between 330 and 350 °C. Mg-Al oxide-supported Ni catalyst also displayed better performance than Ni/MgO and Ni/Al₂O₃ catalysts in CO + CO₂ methanation. The stronger interaction between the support and active component led to excellent thermal stability during the CO + CO₂ methane reaction. Such a catalyst achieved a 98.4% CH₄ yield at 250 °C and maintained a 95.2% CH₄ yield at 700 °C for 8 h [57].

In pursuit of further improvement of the anti-coke ability of (Ni,Mg,Al)-LDH-derived catalysts, some dopants were introduced. La adulteration of Mg-Al-Ni LDH-derived catalysts can form a periclase-like structure and new medium strength basic sites, promote the CO₂ adsorption capacity of the catalysts, soften the interaction between Ni-species and the LDH matrix and improve CO₂ conversion [58,59]. Furthermore, Wierzbicki et al. [59] investigated the effect of the La incorporation method: Ni₂₁La_{0.4}(IE) catalyst prepared by ion-exchange displayed the best catalytic performance and achieved ~80% CO₂ conversion at 300 °C, while the impregnation led to a decrease in the amount of medium strength basic sites, while the catalytic performance of Ni₂₁La_{1.1}(IMP) had no obvious advantage compared with the Ni₂₁ catalyst. In Nizio et al.'s [60] survey of LDH-derived materials, Ce or Zr adulteration cannot improve the catalytic activity, even though the addition of Ce or/and Zr improved the total basicity. In the hybrid plasma-catalytic methanation, the HTNi catalyst exhibited its activity around 80% conversion at 110 °C, whereas only at relatively high temperatures, Ce-promoted catalysts can show interestingly high activities. Moreover, the author thought the medium-sized zero-valent Ni crystallites of non-promoted HTNi (15 nm) catalyst seemed to be more active during off plasma methanation than far too small ones (8.1 nm of HTNi-CeZr), whereas the influence of the basicity of catalysts on their activity remains relatively unclear. However, plasma-assisted Ni-Ce-LDH-P synthesized catalyst reported by Xu et al. [61] in 2017 exhibited better performance compared to HTNi-Ce; Ni-Ce-LDH-P achieved almost 75% CO₂ conversion at 270 °C due to the smaller Ni size, better Ni dispersion and higher alkalinity, whereas Ni-Ce-LDH-C catalyst exhibited the same CO₂ conversion at 300 °C. Likewise, characterization results revealed that the precursor of Ni-Ce-LDH-P catalyst presented a lamellar shape, implying the formation of chemical bonds among Ni, Ce and Al (from Al₂O₃). Actually, it was the chemical bonds that improved the dispersion of Ni crystal and the interaction between Ni and γ-Al₂O₃. Meanwhile, the plasma technology with a relatively low temperature prevented the sintering and agglomeration of Ni during the preparation process.

When the thickness of the material was reduced to the atomic monolayer, the electron density increased, which benefited the high-speed transfer of carrier in the material. This property enabled two-dimensional materials to exhibit great potential in heterogeneous catalysis [62]. Single-layer LDHs (SL-LDHs) drew much more attention recently because of their high performance as energy materials, such as exfoliated NiCo, CoAl and NiFe LDHs [63]. Ren et al. [64] prepared a Ru-loaded ultrathin LDH through ultrasonic exfoliated commercial LDHs in 2016, and the AFM (atomic force microscopy) image showed that the thicknesses of these ultrathin structures were around 8 Å, which nearly corresponds to a single basal spacing of the LDH crystals (Figure 3). The as-prepared catalyst had similar wrinkles to

graphene, and curls existed at the edge and exhibited almost monodispersed Ru nanoparticle or small Ru-nanoparticle aggregates. Ru@FL-LDHs catalyst had the strongest light absorption and exhibited an excellent catalytic performance. Ru@FL-LDHs achieved the highest CO₂ conversion of about 96.3% and 99.3% of selectivity toward the CH₄ in photocatalytic CO₂ methanation.

In conclusion, LDH-derived Ni catalysts were more favorable than traditional impregnated catalysts, while their study in the methanation reaction was limited. As promising catalysts for the methanation reaction, more attention should be paid to future improvement of the catalyst activation and stability, and the reaction mechanism of this kind of catalyst is also worthy of research. Catalytic performance of CO₂ methanation for different catalysts in different works were summarized in Table 2.

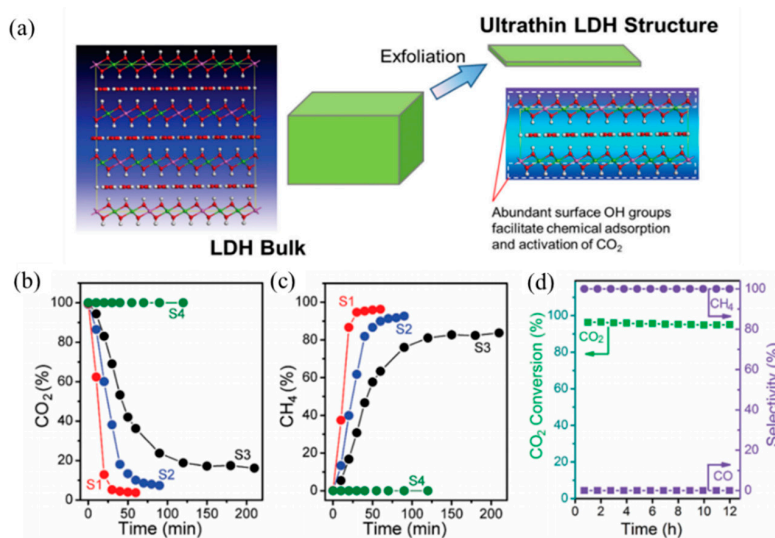


Figure 3. (a) Schematic presence of the formation of the ultrathin LDH structure and (b–d) the catalytic performance of Ru@FL-LDHs [64].

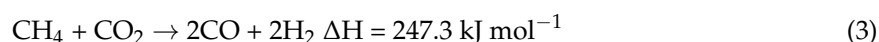
Table 2. Catalytic performance of CO₂ methanation for different catalysts in different works.

Catalyst	Ni (wt %)	T (°C)	Pressure (MPa)	GHSV (mL g ⁻¹ h ⁻¹)	CO ₂ Conversion (%)	CH ₄ Selectivity (%)	Ref.
Ni/Mg-Al	59	330	0.1	66,000	74	–	[56]
Ni-Al 12	76	300	0.1	20,000 h ⁻¹	86	86 (yield)	[21]
NiFeAl-(NH ₄) ₂ CO ₃	30	220	1	9600	58.5	99.5	[55]
Ni ₂₁ La _{0.4} (IE)	21	300	–	12,000 h ⁻¹	80	99.4	[58]
HTNi	20	150	0.1	20,000 h ⁻¹	80	80 (yield)	[60]
Ni-Ce-LDH-P	~4	270	–	60,000	75	100	[61]

3. Methane Reforming

3.1. Dry Reforming of Methane

Dry reforming of methane (DRM) is a critical method for obtaining added-value products from CO₂ and an effective way to utilize these two greenhouse gases. LDHs are also widely investigated in dry reforming of methane (Figure 4) [6,7]. The equation for the dry reforming of methane (DRM) is as follows [21]:



Likewise, two reaction mechanisms of DRM have been surveyed. One mechanism was the Eley–Rideal-type mechanism [65,66]. Methane is firstly adsorbed on the metal and decomposed to H₂

and adsorbed carbon. Then, the adsorbed carbon is reacted directly with CO₂ to yield CO. The equation is as follows:



Additionally, as an alternative reaction mechanism [67–70], methane was decomposed on the metal and produced surface CH species and hydrogen; carbon dioxide molecules decomposed to CO; and oxygen (O(s)) adsorbed at the same time. Afterwards, adsorbed oxygen and CH species reacted to give CO and H₂. The equation is as follows:

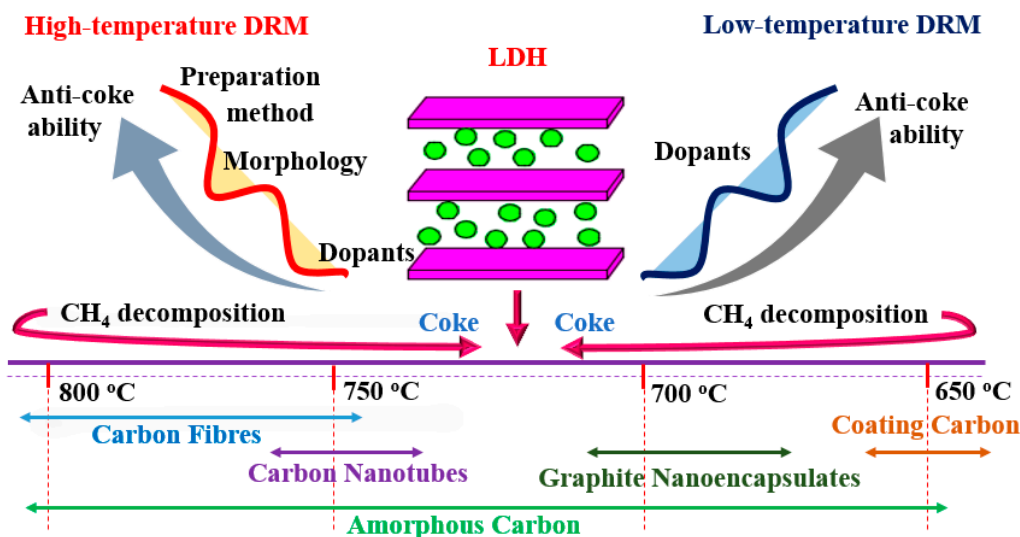


Figure 4. The application of LDHs in dry reforming of methane. DRM, dry reforming of methane.

3.1.1. High Temperature Dry Reforming of Methane

Noble metals like Ru reflected excellent catalytic performance and anti-coke deposition ability in the DRM reaction. Supports have great influence on the dispersion of the active component Ru. Ru metal dispersed on different supports followed the order: Ru/Mg₃(Al)O > Ru/MgO > Ru/MgAl₂O₄ > Ru/γ-Al₂O₃. Ru/Mg₃(Al)O catalyst showed higher catalytic performance due to the strong base intensity of support and more surface Ru⁰ atoms, which ascribed to Mg(Al)O mixed oxide's unique properties, including memory effect, low crystallinity and its strong interaction with Ru [71]. Ru/Mg₃(Al)O catalyst displayed an 84% CH₄ conversion during the 30-h stability test without any deactivation.

Even though noble metal-based catalysts exhibited excellent catalytic performance, industrial applications were limited due to the high cost. Ni was a suitable active catalyst component when taking catalytic performance and cost into consideration. In 1988, Bhattacharyya et al. [72] investigated the performance of LDH-derived catalysts in CO₂ reforming of methane. Compared with commercial Ni/Al₂O₃ catalysts, the LDH-derived Ni₄Al₂O₇ catalyst showed identical performance at 815 °C and 2.07 MPa. LDH-derived catalysts had superior stability and a coke-resistant ability according to aging studies, and the LDH-derived Mg₅NiAl₂O₉ catalyst exhibited the highest CH₄ conversion of 95.8% under operation conditions at 850 °C, 0.67 MPa, GHSV = 14,400 h⁻¹ and CO₂/CH = 1.25; while

Touahra et al. [73] discovered that Ni/Al = 2 was optimal for Ni-Al LDH-derived catalysts due to the low Ni⁰ crystallite size and high stability of the support (NiAl₂O₄).

Consequently, when Mg was introduced to Ni-Al LDHs, the catalytic performance and anti-coke ability of the catalyst improved. Mette et al. [74–76] found that Ni/MgAlO_x catalyst has good anti-coke ability, and the catalytic performance revealed no decrease in performance after 19 times of cycling because nickel aluminate overgrowth on the Ni particles blocked all extended metallic Ni sites, which were nucleation centers for carbon formation. As reported by Lopez et al. [77], the catalytic properties of Ni-Mg-Al catalysts were more affected by the M^{II}/M^{III} ratio compared with the Ni/Mg ratio. When M^{II}/M^{III} was maintained, the catalyst activity was related to the nickel crystal size and Ni/Mg ratio, while selectivity suffered little from the Ni/Mg ratios. This notwithstanding, when Ni/Mg was constant, the catalyst activity was strongly affected and decreased as the M^{II}/M^{III} ratio decreased. Besides, Zhu et al. [78] showed that NiMgAl catalyst with a Mg/Al ratio of 1 displayed the best activity and stability during the DRM reaction, and it was the formation of LDH precursors and MgNiO₂ that played the key role in stabilization. Interestingly, Li et al. [79] demonstrated that the performance of Ni/Mg(Al)O catalyst decreased at the beginning due to the MgO film surrounding the Ni particles; however, the catalyst was renewed after MgAl₂O₄ spinel-like phase formation. The HT-700 catalyst reached approximately 95% CH₄ conversion after 500 h of reaction and maintained for 1500 h. In 2016, Buelens et al. [80] developed a “super-dry” CH₄ reforming through Le Chatelier’s principle reaction (Figure 5): Ni/MgAl₂O₄ was used as the catalyst during the “super-dry” CH₄ reforming. Fe₂O₃/MgAl₂O₄ was used as the solid oxygen carrier, which oxidized CH₄ into CO₂ and H₂O. Meanwhile, the Fe₂O₃ reduced to Fe; CaO/Al₂O₃ was used as the CO₂ sorbent, which formed CaCO₃ and then decomposed into CaO and CO₂, and CO₂ reduced to CO by Fe through a redox reaction. “Super-dry” CH₄ reforming also resulted in a very low exergy destruction per mole CO₂ converted; the exergy destruction for CO₂ conversion was up to 25–50% lower as compared with that of conventional DRM. “Super-dry” CH₄ reforming can result in higher CO production and showed both practical and economic benefits compared with conventional dry reforming.

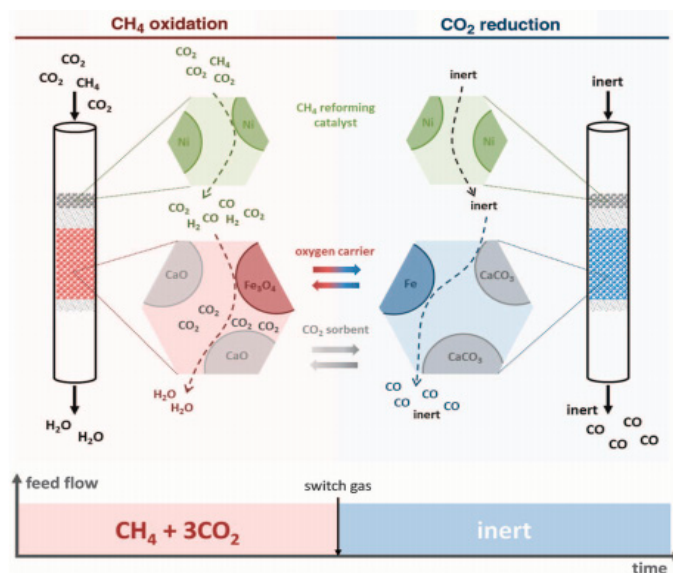


Figure 5. Schematic representation of the “super dry” reforming process [81].

Besides the classic co-precipitation method, other methods also have been employed to prepare high efficiency Ni/Mg/Al LDH-derived catalysts. Meanwhile, Shishido et al. [81] investigated the influence of the preparation method on the catalytic performance of Ni/Mg-Al catalyst. Likewise, the solid phase crystallization (spc) method can promote Ni²⁺ replacement of the Mg²⁺ site in LDH, resulting in the formation of highly dispersed 7% Ni metal particles, while the Ni dispersion of

imp-Ni/Mg-Al was 4.8% (prepared by impregnation method). The catalyst spc-Ni/Mg-Al exhibited a slightly better catalytic performance than imp-Ni/Mg-Al at 800 °C. In addition, Chai et al. [82] developed a FeCrAl-fiber-structured nanocomposite NiO-MgO-Al₂O₃ catalyst in one step, using a γ -Al₂O₃/water interface-assisted method, as shown in Figure 6. The as-obtained catalyst exhibited excellent stability due to Ni nanoparticles being uniformly nested in MgO-Al₂O₃ nano-sheet composites after reducing of the catalyst. Difficult carbon deposition was the main cause for catalyst deactivation, and the deactivation rate was significantly decreased as compared with the Ni/Al₂O₃ catalyst. The NiO-MgO-Al₂O₃ catalyst achieved a CH₄ conversion of 91% at 800 °C with a GHSV of 5000 mL g⁻¹ h⁻¹, CH₄/CO₂ = 1.0/1.1. In situ growth of LDH on γ -Al₂O₃ is also an effective way to prepare DMR catalysts. The NiMgAl-LDO/ γ -Al₂O₃ catalyst has a small Ni nanoparticles size, a strong metal-support interaction and finely-tailored surface basicity. The NiMgAl-LDO/ γ -Al₂O₃ catalyst achieved an 80.7% CH₄ conversion at 700 °C and showed outstanding stability during the 48-h test [83]. Zhang et al. [84] reduced LDH by atmospheric cold plasma jet, and the as-obtained C-LDHs/ γ -Al₂O₃ catalyst can avoid the side-reaction in CO₂-CH₄ reforming, leading to better carbon deposition resistance. C-LDHs/ γ -Al₂O₃ catalyst achieved the same CH₄ conversion of 98% as Ni/MgO/ γ -Al₂O₃ catalyst at 800 °C, but had higher H₂ selectivity.

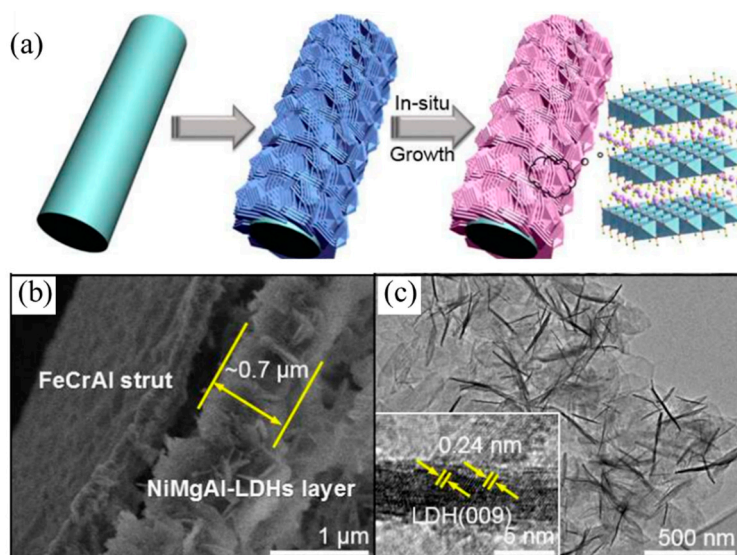


Figure 6. (a) Schematic of microfibrous-structured NiO-MgO-Al₂O₃ nano-sheets grown on FeCrAl-fiber felt and (b) SEM image and (c) TEM image of NiMgAl-LDHs/FeCrAl-fiber-900 [82].

Besides, the main challenge for NiMgAl LDH-derived catalysts was carbon deposition, and many efforts have been made to overcome this obstacle, such as utilizing metal adulation and changing the morphology of the catalyst. Noble metal Rh as a promoter for Ni catalysts can improve the catalyst activity; Rh adulation increased the amount of reducible Ni and promoted the dispersion of Ni. In addition, the presence of Rh probably led to Ni segregation with time on stream and generated carbon deposition due to Rh having favorable CH₄ decomposition [85]. Moreover, Zr adulation to LDH can form periclase-like mixed oxide and rearrangement of Ni particles during the DRM reaction. The HNiZr₃ catalyst exhibited the highest coking resistance properties due to Zr species in the lattice of periclase-like mixed oxide, resulting in small Ni crystallites, which are inactive in direct methane and Boudouard reaction oxides. Yet, Zr adulation decreased the activity, and the CH₄ conversion of HT-25Ni catalyst was 40% and 23% for HTNi-Zr catalyst [86]. La as a promoter can improve nickel metal dispersion and increase the total amount of basic sites and surface Ni content [87]. With 1.1 wt % La adulation, the catalyst properties vary as the Mg/Al molar ratio changes, and the higher Mg/Al molar ratio enhanced the catalyst stability with fewer carbon deposition, but decreased

activity. The best stability was achieved at Mg/Al = 3 during a 120-h test, and the hydro-magnesite phase was formed with a Mg/Al molar ratio of four [88–91].

Ce as a promoter has been revealed by Daza et al. [92–94], who explored two adulteration methods. Ce promoted by the co-precipitation method at constant pH formed mixed reducible phases of the NiO-MgO (periclase) type and CeO₂ (fluorite), and the as-obtained catalyst exhibited better performance than the un-promoted catalyst. OM₂ (Ce-NiMgAl-LDO) catalyst with 14.9% CeO₂ displayed about a 75% CH₄ conversion during the 200-min reaction, and the CO₂ conversion was also about 10% higher than that of OM₁ (NiMgAl-LDO) catalyst, which contained no CeO₂. Further study revealed that Ce and Mg had a synergic effect on the CO₂ adsorption capacity of the solids, promoted the basicity of oxides and enhanced their catalytic activity in CO₂ reforming of methane. However, high loads of Ce decreased the superficial area of the solid and favored the formation of free NiO, which had a negative impact on the selectivity and increased the formation of coke. The fact-finding of Djebbari et al. [95] insinuated that the NiMgCe catalyst was a very stable, and a poorly-reducible mixed oxide phase was formed with Ce adulteration, which inhibited the catalysts' catalytic performance. Besides, the Ce addition affected the catalytic performance. Ren et al. [96] unveiled that Ce introduced through the incipient impregnation method showed higher Ce³⁺ content and appropriate interactions between Ni and NMA compared with catalyst prepared by the co-precipitation method. Daza et al. [97] also revealed that with Ce introduced by partial reconstruction, the as-prepared catalyst formed periclase and fluorite mixed phases after the calcination, and the reconstruction took place at the external edges of the oxide granules. Ce presented an improvement in the degree of reduction of Ni, the amount and strength of the basic sites. With Ce loading increased, no obvious considerable differences in the catalytic activity and selectivity were perceived, but the anti-coke ability was improved. The optimal amount of Ce doping was 3 wt %, and OM₃ (Ce-NiMgAl-LDO) catalysts with (Ni + Mg)/Al = 3 achieved a 90.3% CH₄ conversion at 700 °C, with the CO₂/CH₄/He ratio of 20/20/60 and weight hourly space velocity (WHSV) = 48 L g⁻¹ h⁻¹.

Additionally, the anti-coke ability can also be improved through incorporating carbon in the Ni-based catalyst. In 2017, Jin et al. [33] used sucrose as the carbon source to incorporate carbon in the Ni-based catalyst, and carbon incorporation formed new mesopores, increased the specific surface area and inhibited Ni particle growth. The as-prepared PC-350-1.8 (pretreated catalyst) catalyst exhibited relatively lower initial conversions of CH₄ and CO₂ than pure Ni-LDO catalyst, but showed excellent anti-coke ability. The R-C-350-1.8-800 catalyst was obtained by removing the upper carbon from PC-350-1.8 catalyst, displaying 10% higher CH₄ conversion and showing slightly lower carbon deposition.

Besides transition elements and rare-earth elements, the advantage of the coke resistance ability changed the morphology of the catalysts and can also promote the anti-carbon deposition ability. Du et al. [98] synthesized monolithic Ni-Mg-Al LDH catalyst nanosheets via in situ growth on Al wires. The as-prepare catalyst showed a hierarchical porous structure, and the oxide nanosheets were arranged as a dense film on the aluminum substrate. Monolithic catalysts showed strong metal-support interactions and strong basic sites compared with traditional Ni-MgO-Al₂O₃ catalysts. The monolithic catalysts have also displayed excellent sintering resistance and anti-carbon deposition ability, and coke deposition on the monolithic catalysts was one third that on the traditional catalysts. Du et al. [99] also developed a modular catalyst by combining the Ni-MgO-Al₂O₃ mixed oxide nanoplates with the mesoporous SiO₂ coating, the as-prepared NiMgAl-LDH@m-SiO₂ catalyst core shell structure (Figure 7) and the dual confinement effects: The first confinement was MgO, which can promote embedded Ni NP dispersion and enhance the chemisorption ability of CO₂, as well as restrain the carbon deposition and Ni NP aggregation. The second confinement resulted from the mesoporous SiO₂ shell, which exhibited another "confinement effect". These two confinement effects can reinforce each other, which enabled the modular catalysts to show excellent anti-coke and sintering resistance ability. IR-NiMgAl-LDH@m-SiO₂ achieved a 90% CH₄ conversion at 800 °C, much higher than that of the IM-NiMgAl-LDH@m-SiO₂ (~55%) catalyst obtained by the impregnation method.

González et al. [100] made a Ni-Mg-Al nano-spheroid oxide catalyst through the sol-gel method, and this nano-spheroid oxide catalyst with 15 wt % Ni achieved a 95% CH₄ conversion at 800 °C and showed excellent long-term stability. Amorphous carbon formed on the nano-spheroid catalyst surface during the reaction, which seemed not to be detrimental to this reaction. Encapsulation of carbon is the main culprit in the nickel-containing catalyst's deactivation, because the nickel crystallites are encapsulated by the carbon. However, for this nano-spheroid catalyst, the majority of the carbon was amorphous, and a few seeds of encapsulated carbon benefited from the good conformation of the active sites formed by the nano-crystalline structure of the mixed oxides Mg(Al,Ni)O. In this regard, combining Mg-Al mixed oxides with SBA-15 is also an effective way to improve the anti-coke ability. Zuo et al. [101] found that the catalyst whose metal oxides were calcined two times showed excellent anti-carbon deposition and catalytic stability, due to the strong metal-support interaction and the channel local effect of SBA-15. The SH-550 (SBA-15 added to the hydrotalcite suspension during the preparation) and HS-550 (hydrotalcite added to the SBA-15 suspension during the preparation) catalysts, for which the metal oxides have been calcined two times, achieved almost an 85% CH₄ conversion and maintained excellent stability at 800 °C. For the HS-550 catalyst, the Ni⁰ particles were isolated from one another, so that the clustering of Ni, which is necessary for coke formation, was prevented. In addition, the HS-550 catalyst contained two nickel species: Ni⁰ and NiO; the coexistence of these two species favored the high catalyst activity reported by Damyanova et al. [102].

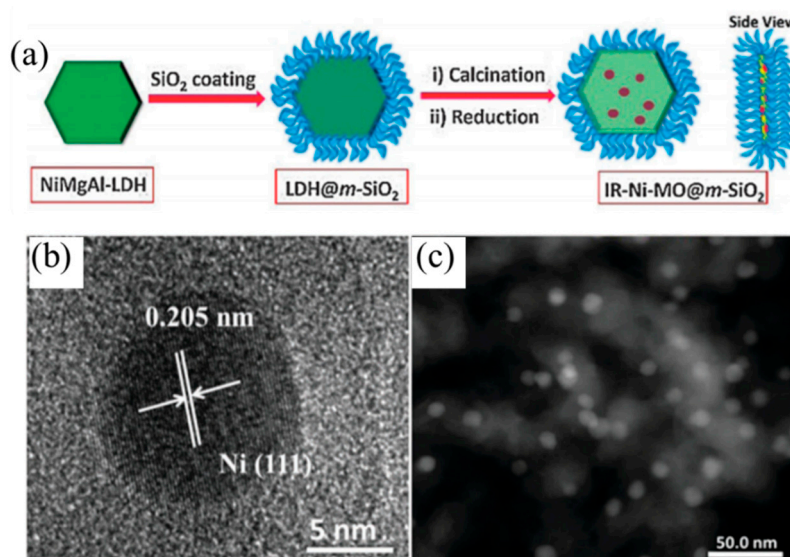


Figure 7. (a) Schematic illustration of the preparation process of the modular catalysts. (b) TEM image and (c) HAADF-STEM image of the modular catalysts [99].

Furthermore, Co was also an active component of DRM reforming, and Co containing LDH has been used as the DRM catalyst. Liu et al. [103] discovered that the catalytic activity, stability and coke resistance of Co/MgAl increased with the increase of Co loading, and the 12% Co/Mg₃Al catalyst showed much higher catalytic stability and much less coke deposition at 600 °C as compared to the 12% Ni/Mg₃Al catalyst, which may be attributed to the higher affinity of Co for oxygen species; in addition, Co has a higher interaction with support. The results suggested that Co has the potential compared to Ni to be an active catalyst in the CH₄-CO₂ reforming reaction. In Gennequin et al.'s study [104], the Co₂Mg₄Al₂HT500 catalyst exhibited better stability as compared with the Co₄Mg₂Al₂HT500 catalyst, though the Co₂Mg₄Al₂HT500 catalyst has a lower initial activity. The Co₆Al₂HT500 catalyst showed comparable catalytic performance to the Co₂Mg₄Al₂HT500 catalyst during the stability test, while Co₆Al₂HT500 showed a larger amount of deposited carbon. After the reaction, three catalysts exhibited a weight decrease corresponding to carbon oxidation following the order: Co₆Al₂HT500

(−52%) > Co₄Mg₂Al₂HT500 (−23%) > Co₂Mg₄Al₂HT500 (−5.5%). Mg oxides could inhibit coke deposition via adsorbed CO₂ species on the basic site and afterwards react with the deposited carbon by the reverse Boudouard reaction. The Co₂Mg₄Al₂HT500 catalyst has a higher Mg content, thus showing excellent anti-coke deposition stability. It could be concluded that for the reaction of the dry reforming of methane, the catalytic performances of Co_xMg_yAl₂HT500 solids have a great relation to Co and Mg content. Gennequin et al. [105] used the “memory effect” of LDHs to impregnate the 1 wt % Ru into Co_xMg_yAl₂, and the as-obtained catalyst exhibited better performance than the conventional impregnation method in the temperature region of 450–750 °C. Regarding this, small amounts of Ru can promote the reducibility of cobalt catalysts and enhance the stability of the catalysts via decreased carbon formation; the catalyst obtained by the “memory effect” generated both metallic and basic sites, which are favorable for the dry reforming reaction of methane.

Moreover, Ni-Co bimetallic LDHs were prepared by the in situ synthesized method on the surface of γ -Al₂O₃. The as-obtained catalysts showed a strong interaction between the active component (Ni and Co) and the catalytic support [106]. However, Tanios et al. [107] discovered that the Ni and Co synergistic effect greatly improved the catalytic properties and prevented carbon formation. The 1Co-2Ni-LDH catalyst exhibited the best catalytic performance and resulted in the least coke, achieving a 98.3% CH₄ conversion that decreased to 1.7% after 50 h of reaction at 800 °C, much higher than that of Co/ γ -Al₂O₃, which resulted in a 56.2% CH₄ conversion and complete deactivation after the 50-h test; while the optimal Co/Ni ratio was one when using aluminum nitrate as the trivalent ion source.

3.1.2. Low Temperature Dry Reforming of Methane

The DRM reaction was always performed at high temperatures to obtain a better performance, whereas LDHs as the catalyst precursors for low temperature dry reforming of methane were studied by Debek et al. [108]. Ni-Al LDH was firstly used as the catalyst for the dry reforming of methane. The HT-NiAl catalyst reduced at 900 °C exhibited a 48% CH₄ conversion and about a 55% CO₂ conversion, higher than that of the HT-NiAl catalyst reduced at 550 °C, due to the reduction temperature of 550 °C not being sufficient to reduce all of the nickel species to being metallic. Moreover, the side reaction of CH₄ decomposition occurring due to an excess of H₂ was observed, and a ca. 30% conversion of methane was obtained by CH₄ on decomposition catalysts reduced at 550 and 900 °C, which evinced that methane decomposition strongly influences the overall process; in addition, the CH₄ decomposition was not influenced by the temperature of the catalyst's pre-treatment.

As the active component, the incorporation method and the content of Ni have a great effect on the DRM reaction. Higher values of CH₄ and CO₂ conversions were obtained for the sample (HTNi) prepared by the co-precipitation method with 63.47 wt % Ni content. About a 55% CH₄ conversion was obtained at 550 °C for the HTNi catalyst, and additional catalytic tests were performed on CH₄ decomposition on the sample HTNi at 550 °C with a feed gas of CH₄/Ar = 2/8. However, HTexNi catalyst with 0.78 wt % Ni displayed higher activity per gram of active material, due to the formation of small Ni NPs or aggregates of nickel oxide on the catalyst surface [109]. Ni particle size increased with Ni content increasing, and dry reforming of methane and direct methane decomposition showed increased methane conversion. Methane decomposition and carbon formation may occur, especially in the presence of catalysts that contain Ni in considerable amounts, and the catalysts with different Ni contents had the same catalytic performance trend as the DRM reaction. Thus, methane decomposition at low temperatures can be controlled by decreasing the Ni particle/crystal size [110].

Because the side reaction of methane decomposition was inevitable during the DRM reaction, methane decomposition led to carbon deposition and catalyst deactivation. Daza et al. [97] found that Ce-promoted catalysts had excellent coke resistance ability. Debek et al. investigated the route cause for this phenomenon. Bigger Ni crystallites on the catalysts with the highest Ni content promoted direct CH₄ decomposition and accelerated catalyst deactivation. Ce-promoted Ni-containing LDH suppressed the side reaction of CH₄ decomposition due to its high basicity enhanced CO₂ adsorption

and excellent ability to oxidize the already formed carbon deposits, whereas too high a loading of ceria had a negative effect during the overall process due to the formation of free NiO [111].

Meanwhile, Zr doping can further promote the coke resistance ability of catalyst and substantially restrain the extensive formation of fishbone-type carbon nanofibers. With the adulteration of Zr, the CH₄ conversion decreased, but Zr considerably inhibited methane's direct decomposition, favored methane reaction with CO₂ (DMR reaction), together with other important parallel reactions, such as the reverse Boudouard reaction. The HT-25Ni catalyst achieved 48% CH₄ conversion and showed 25% CH₄ conversion at 550 °C; even though both CH₄ and CO₂ conversions of the HTNi-CeZr catalyst were low, almost no carbon was deposited on the catalyst surface during 5 h of DMR reaction [112]. The catalysts with Ce/Zr loading of 0.6 and 0.3 exhibited a high concentration of strong basic sites and, as a consequence, showed higher catalytic activity than the H-ZrCe1.2 catalyst. The obtained results revealed that the guarantee of low carbon deposition was due to the presence of Zr species in the lattice of periclase-like mixed oxides, which besides influencing basicity, also result in the formation of small Ni crystallites, inactive in direct methane decomposition and the Boudouard reaction [113].

Unlike Ce and Zr, La as a promoter can not only improve the anti-coke ability, but also enhance catalytic performance [104]. Side reactions such as methane decomposition were promoted at the same time; however, La can form oxycarbonate species and promote gasification of amorphous carbon deposits, resulting in lower carbon formation during the long-duration isothermal experiments performed at 550 °C. La-NiMgAl-LDO catalyst with 2 wt % La showed a 33% CH₄ conversion at 550 °C, slightly higher than that of the un-promoted NiMgAl-LDO catalyst.

3.1.3. The Types of Carbon Deposition

Carbon deposition is unavoidable during DRM and lead to catalyst deactivation. Different carbon species are formed according to the composition of catalysts and the reaction temperature. Thus, many researchers investigated the types of carbon formed on the catalysts' surface. The main types of carbon were amorphous carbon, graphite, carbon nanotubes (CNTs) and carbon nanofibers (CNFs).

Amorphous carbon reflected no impediment to the DRM reaction [84], while encapsulated carbon was mainly responsible for nickel-containing catalysts' deactivation, because the nickel crystallites were encapsulated by the carbon structures. Simultaneously, Daza et al. [94] also showed that different types of carbon formed at different temperatures. At 750 °C, carbon nanotubes (CNTs) and carbon nanofibers (CNFs) were formed, and the filamentous carbons were well-crystallized, yet displayed many structural defects, which increased the resistivity to fracture and prevented the encapsulation of active sites; while at 700 and 650 °C, carbon species were mainly graphite ribbons, coated carbon, nanoencapsulated graphite and Ni particles embedded inside the carbon were mainly responsible for the catalysts' deactivation. Such types of carbon are deeply sensitive to reaction temperature. Düdler et al. [114] found that CNFs formed at 800 °C, and the formation was suppressed at 900 °C, whereas graphitic carbon formed at 900 °C; thus, CNFs are the most deactivating carbon species.

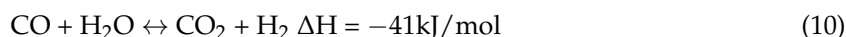
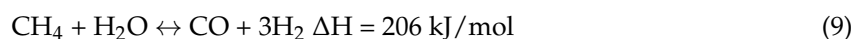
Plenty of works have been done on the application of LDH-derived catalysts to dry reforming of methane, and various LDH-derived catalysts have been developed. Dry reforming of methane was considered as the ideal type of reforming process, the main challenge being catalysts' sintering, carbon deposition and applications to industrial applications. As "super-dry" reforming of methane has been developed, this process obtained higher purity H₂, suppressed side reactions and coke deposition, saved energy compared with traditional dry reforming of methane and was promising for industrial application. Catalytic performance of dry reforming of CH₄ for different catalysts in different works were summarized in Table 3.

Table 3. Catalytic performance of dry reforming of CH₄ for different catalysts in different works.

Catalyst	Ni (wt %)	T (°C)	GHSV (mL g ⁻¹ h ⁻¹)	CO ₂ /CH ₄ Ratios	CH ₄ Conversion (%)	Ref.
Ru/Mg ₃ (Al)O	2	800	60,000	1	84	[71]
NiMgAl-700	10	800	8000	1	95	[79]
Mg ₃ NiAl ₂ O ₉	20	850	7200 h ⁻¹	1.25	95.8	[72]
NiMgAl-LDO/γ-Al ₂ O ₃	9.6	700	24,000	1	80.7	[83]
NiO-MgO-Al ₂ O ₃	13.47	800	5000	1.0/1.1	91	[82]
Ru/Co _x Mg _y Al ₂	–	750	–	1	97	[105]
spc-Ni/Mg-Al	25.1	800	54,000	1	94.5	[81]
Ni/CeO ₂ -ZrO ₂ /MgAl ₂ O ₄	15	850	5000	0.4	81	[115]
La-NiMgAlO	2.8	750	48,000	1	90	[91]
CeO ₂ -Ni/MgAl ₂ O ₄	12	850	5000	0.4	86.2	[116]
Ni/Mg/Al/Ce	48.03	700	48,000	1	80	[92]
Ce-Ni/Mg-Al	50 mol %	700	48,000	92.3	89.4	[94]
Ce-Ni/Mg/Al	50 mol %	800	30,000	100	95	[97]
HS-550	10 (NiO)	800	12,000	1	85%	[101]
HT-NiAl	63.5	550	20,000 h ⁻¹	2	48	[108]
HT-100Ni	58.66	550	20,000 h ⁻¹	1	55	[110]
H-18NiCe	17.9	550	20,000 h ⁻¹	1	41	[111]
HTNi-CeZr	19.3	550	20,000 h ⁻¹	1	25	[112]
NiLaMgAl	15	550	20,000 h ⁻¹	1	33	[103]
HT-NiMgA	5	750	–	1	87.5	[98]
IR-NiMgAl-LDH@m-SiO ₂	5.84	800	–	1	90	[99]
Co ₂ Mg ₄ Al ₂ HT500	25 mol %	800	–	1	96	[104]
Ni-Mg-Al-nano-spheroid	15	800	–	1	95	[100]
12% Co/Mg ₃ Al	12	800	60,000	1	90	[103]
R-C-350-1.8-800	10	800	48,000	1	80	[33]
1Co-2Ni-LDH	5	800	30,000	4/6	98.3	[106]

3.2. Steam Reforming of Methane

Steam reforming of CH₄ is the most common and generally the most economic way to produce H₂. During the steam reforming of methane (MSR) process, there are two main reactions: steam reforming of methane (MSR) and the water gas shift reaction (WGS) [8,9]:



Because of the endothermicity of the reaction, conventional catalysts have the disadvantage of easy carbon deposition, though a high steam to carbon (S/C) ratio can be used to inhibit carbon formation, and the production costs is high. LDHs like catalysts show higher anti-coke and anti-sintering ability than conventional alumina-supported catalysts (Figure 8) [72,117].

Ni/Al LDH-derived catalyst was used as the MSR catalyst. Comas et al. [118] noticed that both reactants CH₄ and H₂O competed for the same active site of Ni during the SMR reaction, and CH₄ conversion presented a maximum or decreased when the water feed concentration increased. When 20 mg of catalyst were used, the CH₄ conversion reached a maximum of 46% at H₂O/CH₄ = 4. Nickel-supported LDHs displayed higher resistance to coke formation than the conventional Ni/γ-Al₂O₃ and Ni/CaO-Al₂O₃ catalysts, due to smaller Ni crystals showing a larger saturation concentration level of filamentous carbon than larger Ni crystals, which lead to the smaller driving force for carbon diffusion [117]. Ni-based LDH-derived catalyst composed by the co-precipitation route exhibited stronger metal-support interaction than that prepared by the incipient wetness method and gave smaller Ni crystals [119]. Catalyst prepared by co-precipitation exhibited high activity and excellent stability: for the 40 Ni/HT catalyst with 40 wt % Ni and Ni dispersion this was 10.8%, showing a 56% CH₄ conversion and no obvious decrease after 25 h of reaction at 650 °C, much higher than that of commercial catalyst, which displayed 1.5% Ni dispersion was and 10% CH₄ conversion. Dehghan-Niri et al. [120] reported that the spatially confined [Ni nanoparticle inside a cage of porous

ribbons had a relatively long distance between themselves, providing significant anti-sintering ability, which brought about a much lower deactivation rate than the commercial Ni catalyst.

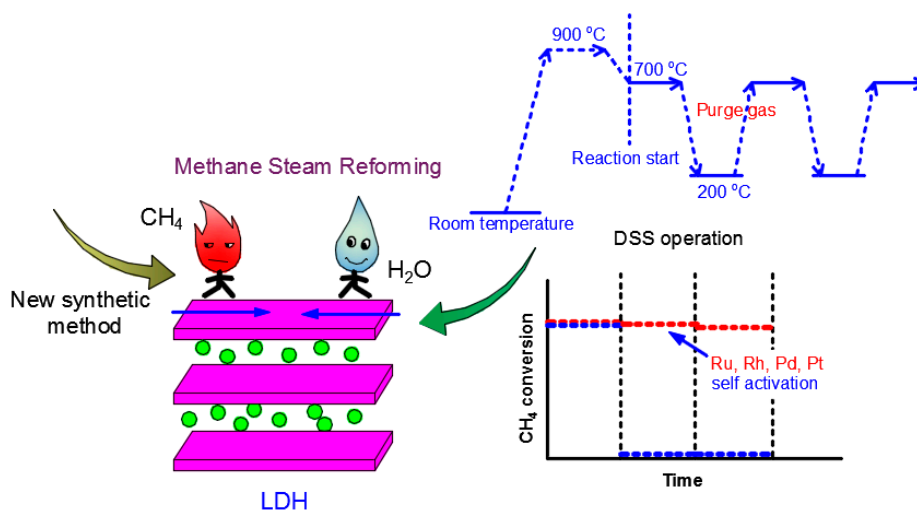


Figure 8. The application of LDHs in steam reforming of methane.

Solid phase crystallization (spc) was also a valuable route to prepare highly efficient and eminent catalyst compared with the incipient wetness method [121]. The as-prepared spc-Ni_{0.5}/Mg_{2.5}-Al catalyst formed NiO-MgO solid solution during the thermal treatment, resulting in well-dispersed Ni metal particles on the catalyst. The spc-Ni/Mg-Al catalyst achieved a 60% CH₄ conversion, and no decline in the activity was observed after 560 h.

In addition, electrodeposition was a new and an eminent method in LDH-derived catalyst preparation. Basile et al. [122] introduced and developed a Ni/Al-NO₃ LDH-derived catalyst through electrodeposition in a single step on FeCr-alloy foams. Furthermore, the catalytic performance was greatly affected by the deposition time. The exHT-1.2-1000 (ex: after calcination) catalyst prepared under 1000 s and -1.2 V showed the best catalytic performance. However, the maximum CH₄ conversion reached the equilibrium value of 67%, due to small and uniform particles of LDHs being deposited on the surface. An eggshell-type Ni/Mg-Al catalyst prepared by replacing a part of the Mg²⁺ by Ni²⁺ using the “memory effect” of LDHs’ structure showed an enhanced catalytic performance compared with impregnated catalyst [123]. The same catalyst formed “worm-like” structures and eventually constituted a dense Ni²⁺ layer and covered the surface of the particles, leading to enrichment of active Ni species. S-spc-Ni_{0.51}/Mg_{2.63}Al (eggshell-type Ni loaded catalysts) catalyst exhibited the best catalytic performance and achieved a 98.1% CH₄ conversion at 800 °C, with a GHSV = 1.8×10^5 mL h⁻¹g⁻¹. Takeguchi et al. [124] analyzed the coke formation of a nickel-based LDH-derived catalyst during steam reforming of methane. The coke deposition rate of the nickel-based LDH-derived catalyst was one third compared with the Ni/Al₂O₃ catalyst because Ni can be oxidized to a Ni-incorporated LDH structure by water-vapor treatment, and the deposited coke was easily removed by the reaction with oxygen in Ni-incorporated LDH [125].

Besides Ni, Ru, Cu and Co were also used as active components. The 1 wt % Ru supported by Co₆Al₂ oxide achieved an ~92% CH₄ conversion at 600 °C, due to the reducible ruthenium and cobalt oxide species at the surface of the support with Ru adulteration [126]. When the reaction temperature reached to 700 °C, the catalyst displayed 100% CH₄ conversion. Cu as an active component showed slightly lower catalytic performance than Ru, but also was an effective active ingredient. Moreover, Homsí et al. [8] studied the influence of copper content on the catalytic performance. The 5Cu/Co₆Al₂ catalyst with 5 wt % Cu showed the best catalytic performance and achieved a 96% methane conversion at 650 °C. With the increasing copper content, the catalyst activity decreased due to the formation of agglomerated and less reactive CuO species. The 5Cu/Co₆Al₂ catalyst can also achieve 100%

methane conversion when the reaction temperature reached 700 °C. Lucr'edio et al. [127] used Co as the active component and studied the influence of the preparation method on the catalytic performance. Catalysts prepared by the traditional technique (traditional co-precipitation method; cobalt nitrate used as the Co ion source) and the anion-exchange method showed good activity, maintaining around 80% conversions during 6 h of reaction. While catalyst prepared by the co-precipitation method (cobalt complex chelate used as the Co ion source) showed an initial fall in conversion, it then remained around 40%, which was caused by cobalt active sites' partial oxidation.

When catalyst is extensively used at the industry scale and operated at daily startup and shutdown (DSS) conditions, the catalyst bed must be purged by a sufficiently inert and an economically viable gas to prevent Ni metal from being oxidized, which could lead to deactivation [128]. Nonetheless, Ohi et al. [129] probed three kinds of purge gas and found that air as the purge gas led to quick deactivation of the oxidized surface metal Ni; spent gas was the most inert for the DSS operation and caused no significant deactivation; as the most convenient purge gas has a great relation to the (Mg + Ni)/Al ratio in Ni/Mg(Al)O catalysts, the most stable operation was achieved with a ratio of 6/1, while the (Mg + Ni)/Al ratio of 3/1 being the most prolific for the steady state operation validated the evident deactivation due to Mg(Al)O being hydrated by steam to form Mg(OH)₂, resulting in the oxidation of Ni metal. Ni_{0.5}/Mg_{2.5}(Al)O catalyst achieved a 91% CH₄ initial conversion, sharply decreasing to 45% under the first shut down, with deactivation after four cycles of the DSS operation [130]. However, when Ru was introduced to Ni_{0.5}/Mg_{2.5}(Al)O, the catalytic performance was effectively preserved under DSS operating conditions. Ru was introduced to the “memory effect” and formed Ru-Ni alloy, which had a strong interaction and effectively suppressed the deactivation. Besides, only 0.05 wt % of Ru loading was enough to suppress the deactivation effectively during the DSS-like operation. In follow-up work [131–133], the author researched the effect of other noble metals such as Rh, Pd and Pt in DSS operating conditions. In addition, Pd was not effective enough compared with Rh addition, since deactivation can be observed. Nevertheless, Rh and Pt with a loading of 0.05 wt % were effective at enhancing the stability of Ni_{0.5}/Mg_{2.5}(Al)O catalyst. The enhancement of stability under DSS operating conditions of Ru, Pt and Rh can be attributed to self-activation of the noble metal-Ni bimetal catalyst: the noble metal rather kept the reduced state during the steam purging and dissociated CH₄ to form hydrogen atoms after the temperature reached 700 °C, then hydrogen atoms migrated to the oxidized Ni species by spillover and reduced them to the active Ni metals.

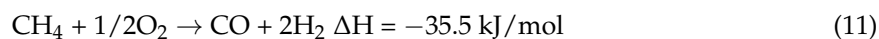
In conclusion, more research should be performed on the LDH-derived catalyst, for it holds promise as catalysts or supports of the SRM catalyst. Since SRM was the most common way to produce H₂, more high-efficiency catalyst that show excellent catalytic performance and anti-coke ability should be explored. Moreover, reaction mechanism also can be researched to help design higher efficiency catalyst. Catalytic performance of steam reforming of CH₄ for different catalysts in different works were summarized in Table 4.

Table 4. Catalytic performance of steam reforming of CH₄ for different catalysts in different works.

Catalyst	Ni (wt %)	T (°C)	Pressure (MPa)	GHSV (mL h ⁻¹ g ⁻¹)	S/C Ratios	CH ₄ Conversion (%)	Ref.
40 Ni/HT	40	650	0.1	–	3	56	[119]
spc-Ni _{0.5} /Mg _{2.5} -Al	~9.8	740	0.1	2890	1.6	60	[134]
exHT-1.2-1000	1.2	900	2	–	1.7	67	[122]
s-spc Ni _{0.51} /Mg _{2.63}	8.2	800	–	180,000	2	98.1	[123]
Ru/Co ₆ Al ₂	1 (Ru)	700	0.1	–	3	100	[126]
5Cu/Co ₆ Al ₂	5 (Cu)	700	0.1	15,000	3	100	[9]
Ae-MgAl-CoY	12.5 mol % (Co)	750	–	49 h ⁻¹	2	80	[127]

3.3. Partial Oxidation of Methane

Catalytic partial oxidation of methane (POM), a mild exothermic process operated at short contact times, offered the greatest potential to synthesis of gas or hydrogen [10]. POM has become the focus of researches due to its obvious advantages, such as mild exothermicity, high energy efficiency and suitable CO/H₂ ratio for methanol synthesis, and could be conducted in small reactors ideal for decentralized applications [11,12]. The equation is as follows:



LDH-derived catalysts are also suitable catalysts for the POM reaction, as shown in Figure 9. Rh-based catalysts are very active in the POM, and Basile et al. [135–138] explored Rh containing LDH-derived Rh/Mg/Al catalysts, which showed better catalytic performance compared with supported Rh/Al₂O₃. Rh/Mg/Al catalysts with a metal ratio of 5.0/71.0/24.0 achieved 91% CH₄ conversion at 750 °C. Rh-based LDH-derived catalysts also have been electro-synthesized on a FeCrAlY foam through the cathodic reduction of a solution containing metal salts and KNO₃, the best catalytic performance being achieved by the catalyst obtained from the HT precursor prepared at −1.3 V for 1000 s. The coating of as-obtained catalyst RhexHT-1.3 pH has a high adhesion to the surface, exhibiting the best catalytic performance with a 90% CH₄ conversion at 750 °C.

Even though Rh catalysts were very active in the POM of methane, the reduced availability and high cost of Rh could make it unsuitable for widespread commercial applications. Ru was less expensive than Rh and was active in the conversion of CH₄. Ballarini et al. [139] unveiled the role of the composition and preparation method in the activity of LDH-derived Ru catalysts in the catalytic partial oxidation of methane. Both Ru dispersion and the interaction with the support decreased as the Ru loading increased and when silicates were present due to RuO₂ segregation, and the 0.25 wt % Ru/Mg/Al-CO₃ catalyst exhibited the best performance due to an enhanced metal-support interaction, carbon resistance and thermal stability. The 0.25 wt % Ru/Mg/Al-CO₃ catalyst achieved 92% CH₄ conversion and almost 100% CO selectivity at 750 °C with a volume ratio of CH₄/O₂/He = 2/1/20. Simultaneously, Velasco et al. [140] also found that with Ru addition, the catalyst showed excellent carbon resistance ability compared to the monometallic nickel catalysts. Harada et al. [141] used Ba_{1.0}Co_{0.7}Fe_{0.2}Nb_{3-δ} (BCFN) dense ceramic supported by Mg-Al compound as an oxygen-permeable membrane for partial oxidation of methane; in 300 h, the oxygen permeation flux BCFN remained greater than 20 mL/(cm² min). With the combination of the oxygen-permeable membrane, Ru 2 wt %/MgAlO_x catalyst afforded the best oxygen permeation performance and achieved initial methane conversion of 85%. This was the first report of such a high flux performance for a reaction in 300 h.

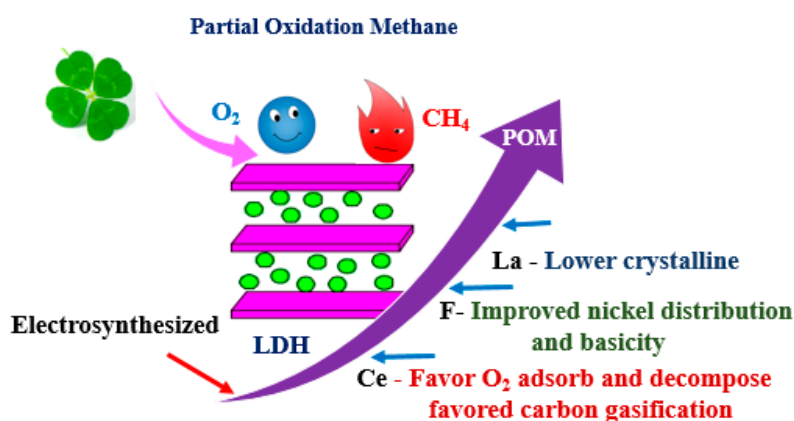


Figure 9. The application of LDHs in partial oxidation of methane. POM, partial oxidation of methane.

Catalysts with lower Ni content activated after a severe reduction treatment can show high stability during the reaction, while catalysts with high Ni content required mild reduction conditions and deactivated rapidly with time-on-stream due to carbon formation. The synergetic effect of Rh and Ni in Rh/Ni LDH-derived catalysts can increase the reducibility of Ni due to Rh being able to catalyze methane reacted with oxygen and increasing the surface temperature at the beginning of the bed [137].

La₂O₃ had a beneficial effect on the nickel dispersion, and the catalysts promoted with lanthanum toward CO₂ reforming methane presented good conversion levels and lower carbon formation than unprompted catalysts. Thus, it was also a potential promoter of the POM reaction. Zhang et al. [10] found that the addition of La lowered the phase crystallization with the formation of small oxide particles. The as-prepared Ni/Mg/Al/La mixed oxides had both high activities and stabilities, the catalyst containing 6.5 mol % La showing the highest performance at 800 °C with a CH₄ conversion of 99%, a CO selectivity of 93% and a H₂ selectivity of 96%, which could be attributed to the presence of highly dispersed nickel and then the resistance to coke formation due to the promotion effect of lanthanum. Besides lanthanum, another rare-earth metal, cerium, also can increase the CO selectivity and decrease the carbon formation rate. With the cerium addition, oxygen was favorable to adsorption and decomposition with respect to these promoted catalysts, which favored the gasification of carbon species [142]. La- and Ce-promoted catalyst showed slightly lower catalytic performance, but achieved a higher CO selectivity than the un-promoted catalyst. The reason for higher selectivity was that La and Ce increased the surface basicity with consequent carbon reduction, which favored the dissociative adsorption of the oxygen in these catalysts [142].

Transition metals and rare-earth metals as promoters have been widely studied; non-metallic elements as the promoter have also displayed a positive effect. Zhang et al. [20] successfully introduced F into Ni-Mg-Al mixed oxide via the high dispersion of MgF₂, which led to the formation of the periclase-type catalyst with a mesoporous structure. Fluorine-modified catalyst showed a low surface area and small Ni particle size, but high-moderate and strong basicity and exhibited excellent catalytic performance for POM without deactivation even after a 120-h run at 800 °C. The high catalytic performance resulted from F⁻ anions improving the homogeneous distribution of nickel and the basicity of the catalyst with high resistance to coking and sintering. Ni/Mg/AlO-F catalyst achieved almost 100% CH₄ conversion at 800 °C.

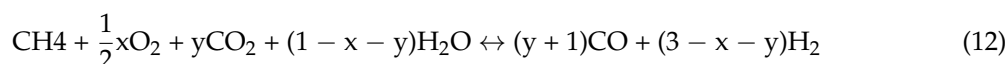
Cobalt has also been used as the active component in the POM reaction. Choudhary and Mamman found that at a molar ratio of CH₄:O₂ = 4:1, the CoO-MgO and NiO-MgO catalysts presented similar results at 700 °C [143]. Additionally, Lucre'dio et al. [142] utilized CoMgAl-Ht as the catalyst for the POM reaction, and the as-prepared catalyst displayed about 50% CH₄ conversion at 750 °C, which reached equilibrium. From existing research, LDH-derived catalysts were propitious for POM. Even though POM required a lower amount of thermal energy compared with DRM and SRM, it required pure oxygen, which may lead to a danger with two combustible reagents. Catalytic performance of steam reforming of CH₄ for different catalysts in different works were summarized in Table 5.

Table 5. Catalytic performance of partial oxidation of CH₄ for different catalysts in different works.

Catalyst	Ni (wt %)	T (°C)	Pressure (MPa)	GHSV (h ⁻¹)	CH ₄ /O ₂ Ratios	CH ₄ Conversion (%)	Ref.
RhexHT-1.3pH	0.2 (Rh)	750	0.1	28,000	2	90	[140]
Ni/Mg/Al/La	21	800	–	–	2	99	[11]
Ru/Mg/AlCO ₃	0.25 (Ru)	750	–	–	2	92	[141]
CoMgAl-Ht	5 mol % (Co)	750	0.1	–	2	50	[142]
Ni/Mg/AlO-F	36 mol %	800	0.1	–	2	100	[26]

3.4. Autothermal Reforming

Autothermal reforming (ATR) is the combination of SMR and POM reactions, and the general reaction for ATR is described in Equation (12) [144]:



It has low-energy requirements due to the opposite contribution of the exothermic methane oxidation and endothermic steam reforming; thus, it can avoid the necessity of a large external supply of heat and the cost of oxygen/nitrogen separation [13]. The combination of these two reactions can improve the reactor temperature, control and reduce the formation of hot spots and avoid catalyst deactivation by sintering or carbon deposition. Moreover, the H₂/CO ratio of syngas produced by ATR has a wider range through manipulating the relative concentrations of H₂O and O₂ in the feed [14,15].

Ni- and/or Rh-containing LDHs have been used as catalysts for autothermal reforming of methane (in the presence or absence of ethane). NiRh alloy particles were formed in NiRh/MgAl, which was enriched in Ni [13]. NiRh/MgAl catalyst hardly catalyzed coke formation during CH₄ autothermal reforming and exhibited excellent stability due to H₂ spillover from Rh in the NiRh alloy against Ni oxidation. NiRh/MgAl catalyst displayed a 93% CH₄ conversion at 500 °C [13]. Luneau et al. [144] tested the long-term stability of a series of catalysts in a six parallel-flow reactor and found that the 5–0.05 wt % Ni-Rh/MgAl₂O₄ catalyst was robust for the autothermal reforming of model biogas, because Rh can effectively promote nickel reduction and prevent bulk oxidation. Likewise, Souza et al. [145] researched Ni-Mg-Al LDH-derived catalysts with varied Ni content for CH₄ autothermal reforming. All catalysts exhibited only MgO-periclase phase X-ray diffraction peaks, suggesting that both nickel and aluminum were well dispersed in the MgO matrix. The performance of LDH-derived catalysts was very similar, with a CH₄ conversion of about 85%, without any apparent deactivation during the stability test at 800 °C. All catalysts achieved a maximum CH₄ conversion of 94% at 900 °C.

Besides the co-precipitation method, the solid-phase crystallization method (spc) was an effective method to prepare high efficiency catalysts and has been used to prepare catalysts for the DRM and SRM reaction. The spc-Ni_{0.5}/Mg_{2.5}Al catalyst with a ratio of Mg/Al of 1/3 showed excellent autothermal reforming performance [146]. Meanwhile, Ni dispersion was further enhanced during the spc preparation process. The spc-Ni_{0.5}/Mg_{2.5}Al catalyst attained almost a 97.5% CH₄ conversion at 800 °C and showed no deactivation during the 50-h stability test. In order to obtain high purity H₂, LDH-derived catalyst also used CO₂ as the sorbent in sorption-enhanced autothermal reforming of methane. Combined with a traditional Ni/MgO catalyst, CH₄ conversion was enhanced to 99.5% with a H₂ purity of 99.5%, higher than that without LDH-derived CO₂ sorbent: 85% and 96%, respectively [147,148].

Autothermal reforming (ATR) was energy saving, and the H₂/CO ratio ranges between one and two [7]. Thus, autothermal reforming was also a good choice to produce syngas. Since LDH-derived catalysts displayed excellent catalytic performance and LDH-derived CO₂ sorbent applied to sorption-enhanced autothermal reforming can produce higher purity H₂, thus more attention should be paid to this research, and new efficient catalysts should be further explored. Catalytic performance of autothermal reforming for different catalysts in different works were summarized in Table 6.

Table 6. Catalytic performance of autothermal reforming for different catalysts in different works.

Catalyst	Ni (wt %)	T (°C)	Pressure (MPa)	GHSV (mL g ⁻¹ h ⁻¹)	CH ₄ /O ₂ /H ₂ O Ratios	CH ₄ Conversion (%)	Ref.
NiRh/MgAl	25	500	–	1,700,000	2/1/2	93	[13]
10NiHT	10	900	0.1	160 h ⁻¹	4/1/2	94	[145]
spc-Ni _{0.5} /Mg _{2.5} Al	16.3	800	–	150,000	2/1/2	~97.5	[146]

4. Conclusions

As conventional 2D materials, LDHs showed small crystal sizes, high surface area, compositional flexibility, memory effect and basic properties, and the as-obtained catalysts displayed large surface area, high thermal stability and a high extent of dispersion of metallic particles after reduction,

so being considered as suitable supports or catalysts for CO/CO₂ methanation and the methane reforming reaction.

(1) Methanation

The NiAl-LDH catalyst with a high Ni loading showed good catalytic performance, but poor anti-sintering ability. The introduction of dopants can effectively decrease the Ni content, improve the reducibility and enhance the interaction between nickel and LDH-based supports, thus further improving the catalytic performance and anti-sintering ability. However, the research of LDH-derived catalysts in the methanation reaction was inadequate. As promising catalysts for the methanation reaction, much further work will be necessary, especially for the single-layer LDHs. The atomic monolayers benefit from the high-speed transfer of the carrier in the material, show similar wrinkles as for graphene and favor the dispersion of the active component as monodispersed nanoparticles, which have great potential in single-atom catalysts.

(2) Methane reforming

Similar to the methanation reaction, the NiAl-LDH catalyst has been also used for the methane reforming reaction, and plenty of work has been performed to restrain the coke deposition. Dopants (Rh, La, Ce, C, etc.) can improve the anti-coke ability of catalysts by improving the active dispersion, enhancing the interaction between the active component and the support and increasing the surface basic sites. Different synthesis methods have also been studied. Besides, the morphology also evidently influences the anti-coke ability, and the monolithic and egg-shell catalysts have shown better anti-coke ability in the dry-reforming reaction. They are also promising catalysts in other kinds of methane reforming.

In addition, the “memory effect” synthesis scheme is also a favorable method for the preparation of highly dispersed LDH-derived catalysts for both methanation and methane reforming reactions. So far, although some dopants have been introduced, the diversification of LDH-derived catalysts is not sufficient, and multicomponent LDH-derived catalysts should be explored.

Acknowledgments: This work was financially supported by the National Natural Science Foundation of China (No. U1203293, 51572029, 51622801), the Program for Changjiang Scholars, Innovative Research Team in University (No. IRT_15R46), and the Program of Science and Technology Innovation Team in Bingtuan (No. 2015BD003).

Conflicts of Interest: The authors declare no conflict of interest.

References

1. Liu, H.; He, D. Recent progress on Ni-based catalysts in partial oxidation of methane to syngas. *Catal. Surv. Asia* **2012**, *16*, 53–61. [[CrossRef](#)]
2. Shan, J.; Li, M.; Allard, L.F.; Lee, S.; Flytzani-Stephanopoulos, M. Mild oxidation of methane to methanol or acetic acid on supported isolated rhodium catalysts. *Nature* **2017**, *551*, 605–608. [[CrossRef](#)] [[PubMed](#)]
3. Craciun, R.; Daniell, W.; Knözinger, H. The effect of CeO₂ structure on the activity of supported pd catalysts used for methane steam reforming. *Appl. Catal. A Gen.* **2002**, *230*, 153–168. [[CrossRef](#)]
4. Wei, J.M.; Xu, B.Q.; Li, J.L.; Cheng, Z.X.; Zhu, Q.M. Highly active and stable Ni/ZrO₂ catalyst for syngas production by CO₂ reforming of methane. *Appl. Catal. A Gen.* **2000**, *196*, L167–L172. [[CrossRef](#)]
5. Elmasides, C.; Verykios, X.E. Mechanistic study of partial oxidation of methane to synthesis gas over modified Ru/TiO₂ catalyst. *J. Catal.* **2001**, *203*, 477–486. [[CrossRef](#)]
6. Zhang, Z.J.; Wang, Q.; Zhu, Y.Q.; Chen, X.Y. Nanoporous graphitic carbon materials: Systematic incorporation of p-/m-/o-nitroaniline as effective redox additives for largely improving the capacitive performance. *Carbon* **2016**, *100*, 564–577. [[CrossRef](#)]
7. Neiva, A.; Gama, A. A study on the characteristics of the reforming of methane: A review. *Braz. J. Pet. Gas* **2010**, *4*, 119–127. [[CrossRef](#)]
8. Micheli, F.; Sciarra, M.; Courson, C.; Gallucci, K. Catalytic steam methane reforming enhanced by CO₂ capture on CaO based bi-functional compounds. *J. Energy Chem.* **2017**, *26*, 1014–1025. [[CrossRef](#)]

9. Homsı, D.; Aouad, S.; Gennequin, C.; Nakat, J.E.; Aboukaıs, A.; Abi-Aad, E. The effect of copper content on the reactivity of Cu/Co₆Al₂ solids in the catalytic steam reforming of methane reaction. *Comptes Rendus Chim.* **2014**, *17*, 454–458. [[CrossRef](#)]
10. Enger, B.C.; Lødeng, R.; Holmen, A. A review of catalytic partial oxidation of methane to synthesis gas with emphasis on reaction mechanisms over transition metal catalysts. *Appl. Catal. A Gen.* **2008**, *346*, 1–27. [[CrossRef](#)]
11. Zhang, J.; Zhao, N.; Wei, W.; Sun, Y. Partial oxidation of methane over Ni/Mg/Al/La mixed oxides prepared from layered double hydroxalcltes. *Int. J. Hydrogen Energy* **2010**, *35*, 11776–11786. [[CrossRef](#)]
12. Freni, S.; Calogero, G.; Cavallaro, S. Hydrogen production from methane through catalytic partial oxidation reactions. *J. Power Source* **2000**, *87*, 28–38. [[CrossRef](#)]
13. Nagaoka, K.; Jentys, A.; Lercher, J.A. Methane autothermal reforming with and without ethane over mono- and bimetal catalysts prepared from hydroxalclte precursors. *J. Catal.* **2005**, *229*, 185–196. [[CrossRef](#)]
14. Liu, S.; Xiong, G.; Dong, H.; Yang, W. Effect of carbon dioxide on the reaction performance of partial oxidation of methane over a LiLaNiO/γ-Al₂O₃ catalyst. *Appl. Catal. A Gen.* **2000**, *202*, 141–146. [[CrossRef](#)]
15. Liu, Z.W.; Jun, K.W.; Roh, H.S.; Park, S.E. Hydrogen production for fuel cells through methane reforming at low temperatures. *J. Power Source* **2002**, *111*, 283–287. [[CrossRef](#)]
16. Liu, Q.; Gao, J.; Gu, F.; Lu, X.; Liu, Y.; Li, H.; Zhong, Z.; Liu, B.; Xu, G.; Su, F. One-pot synthesis of ordered mesoporous Ni–V–Al catalysts for CO methanation. *J. Catal.* **2015**, *326*, 127–138. [[CrossRef](#)]
17. Kok, E.; Scott, J.; Cant, N.; Trimm, D. The impact of ruthenium, lanthanum and activation conditions on the methanation activity of alumina-supported cobalt catalysts. *Catal. Today* **2011**, *164*, 297–301. [[CrossRef](#)]
18. Soltanieh, M.; Azar, K.M.; Saber, M. Development of a zero emission integrated system for co-production of electricity and methanol through renewable hydrogen and CO₂ capture. *Int. J. Greenh. Gas Control* **2012**, *7*, 145–152. [[CrossRef](#)]
19. Metiu, H. CO₂ methanation on Ru-doped ceria. *J. Catal.* **2011**, *278*, 297–309.
20. Zhu, X.; Shi, Y.; Cai, N. CO₂ residual concentration of potassium-promoted hydroxalclte for deep CO/CO₂ purification in H₂-rich gas. *J. Energy Chem.* **2017**, *26*, 956–964. [[CrossRef](#)]
21. Cruz-Hernández, A.; Mendoza-Nieto, J.A.; Pfeiffer, H. NiO–CaO materials as promising catalysts for hydrogen production through carbon dioxide capture and subsequent dry methane reforming. *J. Energy Chem.* **2017**, *26*, 942–947. [[CrossRef](#)]
22. Gao, W.; Zhou, T.; Gao, Y.; Louis, B.; O’Hare, D.; Wang, Q. Molten salts-modified MgO-based adsorbents for intermediate-temperature CO₂ capture: A review. *J. Energy Chem.* **2017**, *26*, 830–838. [[CrossRef](#)]
23. Zhang, Z.; Wang, J.; Huang, L.; Gao, Y.; Umar, A.; Huang, Z.; Wang, Q. The influence of synthesis method on the CO₂ adsorption capacity of Mg₃Al–CO₃ hydroxalclte-derived adsorbents. *Sci. Adv. Mater.* **2014**, *6*, 1154–1159. [[CrossRef](#)]
24. Wang, Q.; Gao, Y.; Zhang, Z.; Duan, L.; Umar, A.; O’Hare, D. Synthesis and characterization of high surface area flower-like ca-containing layered double hydroxides Mg₃–xCaxAl₁₁–NO₃. *Sci. Adv. Mater.* **2013**, *5*, 411–420. [[CrossRef](#)]
25. Xu, Y.; Cheng, C.; Du, S.; Yang, J.; Yu, B.; Luo, J.; Yin, W.; Li, E.; Dong, S.; Ye, P. Contacts between two- and three-dimensional materials: Ohmic, schottky, and p-n heterojunctions. *ACS Nano* **2016**, *10*, 4895–4919. [[CrossRef](#)] [[PubMed](#)]
26. Zhang, J.; Wei, W.; Sun, Y. Fluorine-modified mesoporous Ni–Mg–Al mixed oxides for partial oxidation of methane. *Catal. Lett.* **2010**, *135*, 321–329. [[CrossRef](#)]
27. Dumitriu, E.; Hulea, V.; Chelaru, C.; Catrinescu, C.; Tichit, D.; Durand, R. Influence of the acid–base properties of solid catalysts derived from hydroxalclte-like compounds on the condensation of formaldehyde and acetaldehyde. *Appl. Catal. A Gen.* **1999**, *178*, 145–157. [[CrossRef](#)]
28. Liu, K.; Xu, Y.; Yao, Z.; Miras, H.N.; Song, Y.F. Polyoxometalate-intercalated layered double hydroxides as efficient and recyclable bifunctional catalysts for cascade reactions. *ChemCatChem* **2016**, *8*, 929–937. [[CrossRef](#)]
29. Yao, Z.; Miras, H.N.; Song, Y.F. Efficient concurrent removal of sulfur and nitrogen contents from complex oil mixtures by using polyoxometalate-based composite materials. *Inorg. Chem. Front.* **2016**, *3*, 1007–1013. [[CrossRef](#)]
30. Han, J.; Dou, Y.; Wei, M.; Evans, D.G.; Duan, X. Erasable nanoporous antireflection coatings based on the reconstruction effect of layered double hydroxides. *Angew. Chem.* **2010**, *49*, 2171–2174. [[CrossRef](#)] [[PubMed](#)]

31. Takehira, K. Recent development of layered double hydroxide-derived catalysts—rehydration, reconstitution, and supporting, aiming at commercial application—. *Appl. Clay Sci.* **2017**, *136*, 112–141. [[CrossRef](#)]
32. Cavani, F.; Trifirò, F.; Vaccari, A. Hydrotalcite-type anionic clays: Preparation, properties and applications. *Catal. Today* **1991**, *11*, 173–301. [[CrossRef](#)]
33. Jin, L.; Xie, T.; Ma, B.; Li, Y.; Hu, H. Preparation of carbon-Ni/MgO-Al₂O₃ composite catalysts for CO₂ reforming of methane. *Int. J. Hydrogen Energy* **2017**, *42*, 5047–5055. [[CrossRef](#)]
34. Li, P.; Zhu, M.; Tian, Z.; Han, Y.; Zhang, Y.; Zhou, T.; Kang, L.; Dan, J.; Guo, X.; Yu, F.; et al. Two-dimensional layered double hydroxide derived from vermiculite waste water supported highly dispersed ni nanoparticles for co methanation. *Catalysts* **2017**, *7*, 79. [[CrossRef](#)]
35. Bian, L.; Wang, W.; Xia, R.; Li, Z. Ni-based catalyst derived from Ni/Al hydrotalcite-like compounds by the urea hydrolysis method for CO methanation. *RSC Adv.* **2015**, *6*, 677–686. [[CrossRef](#)]
36. Habazaki, H.; Yamasaki, M.; Zhang, B.P.; Kawashima, A.; Kohno, S.; Takai, T.; Hashimoto, K. Co-methanation of carbon monoxide and carbon dioxide on supported nickel and cobalt catalysts prepared from amorphous alloys. *Appl. Catal. A Gen.* **1998**, *172*, 131–140. [[CrossRef](#)]
37. Zhang, M.; Li, P.; Zhu, M.; Tian, Z.; Dan, J.; Li, J.; Dai, B.; Yu, F. Ultralow-weight loading Ni catalyst supported on two-dimensional vermiculite for carbon monoxide methanation. *Chin. J. Chem. Eng.* **2017**, in press. [[CrossRef](#)]
38. Dai, B.; Wen, B.; Zhu, M.; Kang, L.; Yu, F. Nickel catalysts supported on amino-functionalized MCM-41 for syngas methanation. *RSC Adv.* **2016**, *6*, 66957–66962. [[CrossRef](#)]
39. Li, P.; Zhu, M.; Dan, J.; Kang, L.; Lai, L.; Cai, X.; Zhang, J.; Yu, F.; Tian, Z.; Dai, B. Two-dimensional porous SiO₂ nanomesh supported high dispersed ni nanoparticles for CO methanation. *Chem. Eng. J.* **2017**, *326*, 774–780. [[CrossRef](#)]
40. Al-Fatih, A.; Ibrahim, A.; Fakeeha, A.; Soliman, M.; Siddiqui, M.; Abasaheed, A. Coke formation during CO₂ reforming of CH₄ over alumina-supported nickel catalysts. *Appl. Catal. A Gen.* **2009**, *364*, 150–155. [[CrossRef](#)]
41. Rostrup-Nielsen, J.R.; Pedersen, K.; Sehested, J. High temperature methanation: Sintering and structure sensitivity. *Appl. Catal. A Gen.* **2007**, *330*, 134–138. [[CrossRef](#)]
42. Mohaideen, K.K.; Kim, W.; Koo, K.Y.; Wang, L.Y. Highly dispersed Ni particle on Ru/NiAl catalyst derived from layered double hydroxide for selective CO methanation. *Catal. Commun.* **2014**, *60*, 8–13. [[CrossRef](#)]
43. Rathouský, J.; Schulz-Ekloff, G.; Stárek, J.; Zúkal, A. Supported nickel catalyst from hydroxycarbonate of nickel and aluminium. *Chem. Eng. Technol.* **1994**, *17*, 41–46. [[CrossRef](#)]
44. Kelley, R.D.; Candela, G.A.; Madey, T.E.; Newbury, D.E.; Schehl, R.R. Surface and bulk analysis of a deactivated raney nickel methanation catalyst. *J. Catal.* **1983**, *80*, 235–248. [[CrossRef](#)]
45. Betta, R.A.D.; Piken, A.G.; Shelef, M. Heterogeneous methanation: Steady-state rate of CO hydrogenation on supported ruthenium, nickel and rhenium. *J. Catal.* **1975**, *40*, 173–183.
46. Hwang, S.; Lee, J.; Hong, U.G.; Ji, C.J.; Dong, J.K.; Lim, H.; Byun, C.; Song, I.K. Hydrogenation of carbon monoxide to methane over mesoporous nickel-m-alumina (m = Fe, Ni, Co, Ce, and La) xerogel catalysts. *J. Ind. Eng. Chem.* **2012**, *18*, 243–248. [[CrossRef](#)]
47. Kustov, A.L.; Frey, A.M.; Larsen, K.E.; Johannessen, T.; Nørskov, J.K.; Christensen, C.H. Co methanation over supported bimetallic Ni-Fe catalysts: From computational studies towards catalyst optimization. *Appl. Catal. A Gen.* **2007**, *320*, 98–104. [[CrossRef](#)]
48. Li, Z.; Bian, L.; Zhu, Q.; Wang, W. Ni-based catalyst derived from Ni/Mg/Al hydrotalcite-like compounds and its activity in the methanation of carbon monoxide. *Kinet. Catal.* **2014**, *55*, 217–223. [[CrossRef](#)]
49. Collet, P.; Flottes, E.; Favre, A.; Raynal, L.; Pierre, H.; Capela, S.; Peregrina, C. Techno-economic and life cycle assessment of methane production via biogas upgrading and power to gas technology. *Appl. Energy* **2017**, *192*, 282–295. [[CrossRef](#)]
50. Abate, S.; Barbera, K.; Giglio, E.; Deorsola, F.; Bensaid, S.; Perathoner, S.; Pirone, R.; Centi, G. Synthesis, characterization, and activity pattern of Ni-Al hydrotalcite catalysts in CO₂ methanation. *Ind. Eng. Chem. Res.* **2016**, *55*, 8299–8308. [[CrossRef](#)]
51. Gabrovska, M.; Edreva-Kardjieva, R.; Crişan, D.; Tzvetkov, P.; Shopska, M.; Shtereva, I. Ni-Al layered double hydroxides as catalyst precursors for CO₂ removal by methanation. *React. Kinet. Mech. Catal.* **2012**, *105*, 79–99. [[CrossRef](#)]
52. Rahmani, S.; Rezaei, M.; Meshkani, F. Preparation of promoted nickel catalysts supported on mesoporous nanocrystalline gamma alumina for carbon dioxide methanation reaction. *J. Ind. Eng. Chem.* **2014**, *20*, 4176–4182. [[CrossRef](#)]

53. Westermann, A.; Azambre, B.; Bacariza, M.C.; Graça, I.; Ribeiro, M.F.; Lopes, J.M.; Henriques, C. The promoting effect of ce in the CO₂ methanation performances on niusy zeolite: A ftir in situ/operando study. *Catal. Today* **2017**, *283*, 74–81. [[CrossRef](#)]
54. Tada, S.; Shimizu, T.; Kameyama, H.; Haneda, T.; Kikuchi, R. Ni/CeO₂ catalysts with high CO₂ methanation activity and high CH₄ selectivity at low temperatures. *Int. J. Hydrogen Energy* **2012**, *37*, 5527–5531. [[CrossRef](#)]
55. Hwang, S.; Hong, U.G.; Lee, J.; Seo, J.G.; Baik, J.H.; Dong, J.K.; Lim, H.; Song, I.K. Methanation of carbon dioxide over mesoporous Ni–Fe–Al₂O₃ catalysts prepared by a coprecipitation method: Effect of precipitation agent. *J. Ind. Eng. Chem.* **2013**, *19*, 2016–2021. [[CrossRef](#)]
56. Bette, N.; Thielemann, J.; Schreiner, M.; Mertens, F. Methanation of CO₂ over a (Mg,Al)Ox supported nickel catalyst derived from a (Ni,Mg,Al)-hydrotalcite-like precursor. *ChemCatChem* **2016**, *8*, 2903–2906. [[CrossRef](#)]
57. Fan, M.T.; Miao, K.P.; Lin, J.D.; Zhang, H.B.; Liao, D.W. Mg-Al oxide supported Ni catalysts with enhanced stability for efficient synthetic natural gas from syngas. *Appl. Surf. Sci.* **2014**, *307*, 682–688. [[CrossRef](#)]
58. Wierzbicki, D.; Motak, M.; Grzybek, T.; Gálvez, M.E.; Costa, P.D. The influence of lanthanum incorporation method on the performance of nickel-containing hydrotalcite-derived catalysts in CO₂ methanation reaction. *Catal. Today* **2017**, in press. [[CrossRef](#)]
59. Wierzbicki, D.; Debek, R.; Motak, M.; Grzybek, T.; Gálvez, M.E.; Costa, P.D. Novel Ni-La-hydrotalcite derived catalysts for CO₂ methanation. *Catal. Commun.* **2016**, *83*, 5–8. [[CrossRef](#)]
60. Nizio, M.; Benrabbah, R.; Krzak, M.; Debek, R.; Motak, M.; Cavadias, S.; Gálvez, M.E.; Costa, P.D. Low temperature hybrid plasma-catalytic methanation over Ni-Ce-Zr hydrotalcite-derived catalysts. *Catal. Commun.* **2016**, *83*, 14–17. [[CrossRef](#)]
61. Xu, Y.; Chen, Y.; Li, J.; Zhou, J.; Song, M.; Zhang, X.; Yin, Y. Improved low-temperature activity of Ni–Ce/ γ -Al₂O₃ catalyst with layer structural precursor prepared by cold plasma for CO₂ methanation. *Int. J. Hydrogen Energy* **2017**, *42*, 13085–13091. [[CrossRef](#)]
62. Sun, Y.; Cheng, H.; Gao, S.; Sun, Z.; Liu, Q.; Liu, Q.; Lei, F.; Yao, T.; He, J.; Wei, S. Freestanding tin disulfide single-layers realizing efficient visible-light water splitting. *Angew. Chem. Int. Ed.* **2012**, *51*, 8727–8731. [[CrossRef](#)] [[PubMed](#)]
63. Li, H.; Tran, T.N.; Lee, B.J.; Zhang, C.; Park, J.D.; Kang, T.H.; Yu, J.S. Synthesis of water-dispersible single-layer coal-carbonate layered double hydroxide. *ACS Appl. Mater. Interfaces* **2017**, *9*, 20294–20298. [[CrossRef](#)] [[PubMed](#)]
64. Ren, J.; Ouyang, S.; Xu, H.; Meng, X.; Wang, T.; Wang, D.; Ye, J. Photothermal catalysis: Targeting activation of CO₂ and H₂ over Ru-loaded ultrathin layered double hydroxides to achieve efficient photothermal CO₂ methanation in flow-type system. *Adv. Energy Mater.* **2017**, *7*. [[CrossRef](#)]
65. Mark, M.F.; Maier, W.F. CO₂-reforming of methane on supported Rh and Ir catalysts. *J. Catal.* **1996**, *164*, 122–130. [[CrossRef](#)]
66. Erdohelyi, A.; Cserenyi, J.; Solymosi, F. Activation of CH₄ and its reaction with CO₂ over supported Rh catalysts. *J. Catal.* **1993**, *141*, 287–299. [[CrossRef](#)]
67. Kroll, V.C.H.; Swaan, H.M.; Lacombe, S.; Mirodatos, C. Methane reforming reaction with carbon dioxide over Ni/SiO₂ catalyst: Ii. A mechanistic study. *J. Catal.* **1996**, *164*, 387–398. [[CrossRef](#)]
68. Richardson, J.T.; Paripatyadar, S.A. Carbon dioxide reforming of methane with supported rhodium. *Appl. Catal.* **1990**, *61*, 293–309. [[CrossRef](#)]
69. Solymosi, F.; Kutsán, G.; Erdöhelyi, A. Catalytic reaction of CH₄ with CO₂ over alumina-supported Pt metals. *Catal. Lett.* **1991**, *11*, 149–156. [[CrossRef](#)]
70. Qin, D.; Lapszewicz, J. Study of mixed steam and CO₂ reforming of CH₄ to syngas on mgo-supported metals. *Catal. Today* **1994**, *21*, 551–560. [[CrossRef](#)]
71. Li, D.; Li, R.; Lu, M.; Lin, X.; Zhan, Y.; Jiang, L. Carbon dioxide reforming of methane over Ru catalysts supported on Mg-Al oxides: A highly dispersed and stable Ru/Mg(Al)O catalyst. *Appl. Catal. B Environ.* **2017**, *200*, 566–577. [[CrossRef](#)]
72. Bhattacharyya, A.; Chang, V.W.; Schumacher, D.J. CO₂ reforming of methane to syngas: I: Evaluation of hydrotalcite clay-derived catalysts. *Appl. Clay Sci.* **1998**, *13*, 317–328. [[CrossRef](#)]
73. Touahra, F.; Sehailia, M.; Ketir, W.; Bachari, K.; Chebout, R.; Trari, M.; Cherifi, O.; Halliche, D. Effect of the Ni/Al ratio of hydrotalcite-type catalysts on their performance in the methane dry reforming process. *Appl. Petrochem. Res.* **2016**, *6*, 1–13. [[CrossRef](#)]

74. Mette, K.; Kühl, S.; Düdler, H.; Kähler, K.; Tarasov, A.; Muhler, M.; Behrens, M. Stable performance of Ni catalysts in the dry reforming of methane at high temperatures for the efficient conversion of CO₂ into syngas. *ChemCatChem* **2014**, *6*, 100–104. [[CrossRef](#)]
75. Mette, K.; Kühl, S.; Tarasov, A.; Düdler, H.; Kähler, K.; Muhler, M.; Schlögl, R.; Behrens, M. Redox dynamics of Ni catalysts in CO₂ reforming of methane. *Catal. Today* **2015**, *242*, 101–110. [[CrossRef](#)]
76. Mette, K.; Kühl, S.; Tarasov, A.; Willinger, M.G.; Kröhnert, J.; Wrabetz, S.; Trunschke, A.; Scherzer, M.; Girgsdies, F.; Düdler, H. High-temperature stable Ni nanoparticles for the dry reforming of methane. *ACS Catal.* **2016**, *6*, 7238–7248. [[CrossRef](#)]
77. Perez-Lopez, O.W.; Senger, A.; Marcilio, N.R.; Lansarin, M.A. Effect of composition and thermal pretreatment on properties of Ni–Mg–Al catalysts for CO₂ reforming of methane. *Appl. Catal. A Gen.* **2006**, *303*, 234–244. [[CrossRef](#)]
78. Zhu, Y.; Zhang, S.; Chen, B.; Zhang, Z.; Shi, C. Effect of Mg/Al ratio of NiMgAl mixed oxide catalyst derived from hydrotalcite for carbon dioxide reforming of methane. *Catal. Today* **2016**, *264*, 163–170. [[CrossRef](#)]
79. Li, N.; Shen, C.; Tan, P.; Zuo, Z.; Huang, W. Effect of phase transformation on the stability of Ni–Mg–Al catalyst for dry reforming of methane. *Indian J. Chem.* **2015**, *54*, 1198–1205.
80. Buelens, L.C.; Galvita, V.V.; Poelman, H.; Detavernier, C.; Marin, G.B. Super-dry reforming of methane intensifies CO₂ utilization via le chatelier's principle. *Science* **2016**, *354*, 449–452. [[CrossRef](#)] [[PubMed](#)]
81. Shishido, T.; Sukenobu, M.; Morioka, H.; Furukawa, R.; Shirahase, H.; Takehira, K. CO₂ reforming of CH₄ over Ni/Mg–Al oxide catalysts prepared by solid phase crystallization method from Mg–Al hydrotalcite-like precursors. *Catal. Lett.* **2001**, *73*, 21–26. [[CrossRef](#)]
82. Chai, R.; Fan, S.; Zhang, Z.; Chen, P.; Zhao, G.; Liu, Y.; Lu, Y. Free-standing NiO–MgO–Al₂O₃ nanosheets derived from layered double hydroxides grown onto fecral-fiber as structured catalysts for dry reforming of methane. *ACS Sustain. Chem. Eng.* **2017**, *5*, 4517–4522. [[CrossRef](#)]
83. Xu, Z.; Wang, N.; Chu, W.; Deng, J.; Luo, S. In situ controllable assembly of layered-double-hydroxide-based nickel nanocatalysts for carbon dioxide reforming of methane. *Catal. Sci. Technol.* **2015**, *5*, 1588–1597. [[CrossRef](#)]
84. Zhang, X.; Wang, N.; Xu, Y.; Yin, Y.; Shang, S. A novel Ni–Mg–Al–LDHs/γ-Al₂O₃ catalyst prepared by in-situ synthesis method for CO₂ reforming of CH₄. *Catal. Commun.* **2014**, *45*, 11–15. [[CrossRef](#)]
85. Lucrédio, A.F.; Assaf, J.M.; Assaf, E.M. Methane conversion reactions on Ni catalysts promoted with Rh: Influence of support. *Appl. Catal. A Gen.* **2011**, *400*, 156–165. [[CrossRef](#)]
86. Dėbek, R.; Motak, M.; Galvez, M.E.; Grzybek, T.; Da Costa, P. Promotion effect of zirconia on Mg (Ni, Al)O mixed oxides derived from hydrotalcites in CO₂ methane reforming. *Appl. Catal. B: Environ.* **2018**, *223*, 36–46. [[CrossRef](#)]
87. Yu, X.; Wang, N.; Chu, W.; Liu, M. Carbon dioxide reforming of methane for syngas production over La-promoted NiMgAl catalysts derived from hydrotalcites. *Chem. Eng. J.* **2012**, *209*, 623–632. [[CrossRef](#)]
88. Serrano-Lotina, A.; Martin, A.J.; Folgado, M.A.; Daza, L. Dry reforming of methane to syngas over La-promoted hydrotalcite clay-derived catalysts. *Int. J. Hydrogen Energy* **2012**, *37*, 12342–12350. [[CrossRef](#)]
89. Serrano-Lotina, A.; Daza, L.; Serrano-Lotina, A.; Daza, L. Highly stable and active catalyst for hydrogen production from biogas. *J. Power Source* **2013**, *238*, 81–86. [[CrossRef](#)]
90. Serrano-Lotina, A.; Daza, L. Influence of the operating parameters over dry reforming of methane to syngas. *Int. J. Hydrogen Energy* **2014**, *39*, 4089–4094. [[CrossRef](#)]
91. Serrano-Lotina, A.; Daza, L. Long-term stability test of Ni-based catalyst in carbon dioxide reforming of methane. *Appl. Catal. A Gen.* **2014**, *474*, 107–113. [[CrossRef](#)]
92. Daza, C.E.; Gallego, J.; Moreno, J.A.; Mondragón, F.; Moreno, S.; Molina, R. CO₂ reforming of methane over Ni/Mg/Al/Ce mixed oxides. *Catal. Today* **2008**, *133*, 357–366. [[CrossRef](#)]
93. Daza, C.E.; Moreno, S.; Molina, R. Co-precipitated Ni–Mg–Al catalysts containing Ce for CO reforming of methane. *Int. J. Hydrogen Energy* **2011**, *36*, 3886–3894. [[CrossRef](#)]
94. Daza, C.E.; Gallego, J.; Mondragón, F.; Moreno, S.; Molina, R. High stability of Ce-promoted Ni/Mg–Al catalysts derived from hydrotalcites in dry reforming of methane. *Fuel* **2010**, *89*, 592–603. [[CrossRef](#)]
95. Djebbari, B.; Gonzalez-Delacruz, V.M.; Halliche, D.; Bachari, K.; Saadi, A.; Caballero, A.; Holgado, J.P.; Cherifi, O. Erratum to: Promoting effect of Ce and Mg cations in Ni/Al catalysts prepared from hydrotalcites for the dry reforming of methane. *React. Kinet. Mech. Catal.* **2014**, *111*, 817. [[CrossRef](#)]

96. Ren, H.P.; Song, Y.H.; Wang, W.; Chen, J.G.; Cheng, J.; Jiang, J.; Liu, Z.T.; Liu, Z.W.; Hao, Z.; Lu, J. Insights into CeO₂-modified Ni–Mg–Al oxides for pressurized carbon dioxide reforming of methane. *Chem. Eng. J.* **2015**, *259*, 581–593. [[CrossRef](#)]
97. Daza, C.E.; Cabrera, C.R.; Moreno, S.; Molina, R. Syngas production from CO₂ reforming of methane using Ce-doped Ni-catalysts obtained from hydrotalcites by reconstruction method. *Appl. Catal. A Gen.* **2010**, *378*, 125–133. [[CrossRef](#)]
98. Du, X.; Zhang, D.; Shi, L.; Gao, R.; Zhang, J. Coke- and sintering-resistant monolithic catalysts derived from in situ supported hydrotalcite-like films on Al wires for dry reforming of methane. *Nanoscale* **2013**, *5*, 2659–2663. [[CrossRef](#)] [[PubMed](#)]
99. Du, X.; Zhang, D.; Gao, R.; Huang, L.; Shi, L.; Zhang, J. Design of modular catalysts derived from NiMgAl-LDH@m-SiO₂ with dual confinement effects for dry reforming of methane. *Chem. Commun.* **2013**, *49*, 6770–6772. [[CrossRef](#)] [[PubMed](#)]
100. González, A.R.; Asencios, Y.J.O.; Assaf, E.M.; Assaf, J.M. Dry reforming of methane on Ni–Mg–Al nano-spheroid oxide catalysts prepared by the sol–gel method from hydrotalcite-like precursors. *Appl. Surf. Sci.* **2013**, *280*, 876–887. [[CrossRef](#)]
101. Zuo, Z.J.; Shen, C.F.; Tan, P.J.; Huang, W. Ni based on dual-support Mg–Al mixed oxides and SBA-15 catalysts for dry reforming of methane. *Catal. Commun.* **2013**, *41*, 132–135. [[CrossRef](#)]
102. Damyanova, S.; Pawelec, B.; Arishtirova, K.; Fierro, J.L.G. Ni-based catalysts for reforming of methane with CO₂. *Int. J. Hydrogen Energy* **2012**, *37*, 15966–15975. [[CrossRef](#)]
103. Liu, H.; Wierzbicki, D.; Debek, R.; Motak, M.; Grzybek, T.; Costa, P.D.; Gálvez, M.E. La-promoted Ni-hydrotalcite-derived catalysts for dry reforming of methane at low temperatures. *Fuel* **2016**, *182*, 8–16. [[CrossRef](#)]
104. Gennequin, C.; Safariamin, M.; Siffert, S.; Aboukaïs, A.; Abi-Aad, E. CO₂ reforming of CH₄ over Co–Mg–Al mixed oxides prepared via hydrotalcite like precursors. *Catal. Today* **2011**, *176*, 139–143. [[CrossRef](#)]
105. Gennequin, C.; Hany, S.; Tidahy, H.L.; Aouad, S.; Estephane, J.; Aboukaïs, A.; Abi-Aad, E. Influence of the presence of ruthenium on the activity and stability of Co–Mg–Al-based catalysts in CO₂ reforming of methane for syngas production. *Environ. Sci. Pollut. Res. Int.* **2016**, *23*, 22744–22760. [[CrossRef](#)] [[PubMed](#)]
106. Zhang, X.; Yang, C.; Zhang, Y.; Xu, Y.; Shang, S.; Yin, Y. Ni–Co catalyst derived from layered double hydroxides for dry reforming of methane. *Int. J. Hydrogen Energy* **2015**, *40*, 16115–16126. [[CrossRef](#)]
107. Taniou, C.; Bsaibes, S.; Gennequin, C.; Labaki, M.; Cazier, F.; Billet, S.; Tidahy, H.L.; Nsouli, B.; Aboukaïs, A.; Abi-Aad, E. Syngas production by the CO₂ reforming of CH₄ over Ni–Co–Mg–Al catalysts obtained from hydrotalcite precursors. *Int. J. Hydrogen Energy* **2017**, *42*, 12818–12828. [[CrossRef](#)]
108. Debek, R.; Ribeiro, M.F.G.; Fernandes, A.; Motak, M. Ni–Al hydrotalcite-like material as the catalyst precursors for the dry reforming of methane at low temperature. *C. R. Chim.* **2015**, *18*, 1205–1210. [[CrossRef](#)]
109. Debek, R.; Zubek, K.; Motak, M.; Costa, P.D.; Grzybek, T. Effect of nickel incorporation into hydrotalcite-based catalyst systems for dry reforming of methane. *Res. Chem. Intermed.* **2015**, *41*, 9485–9495. [[CrossRef](#)]
110. Debek, R.; Motak, M.; Duraczyska, D.; Launay, F.; Galvez, M.E.; Grzybek, T.; Costa, P.D. Methane dry reforming over hydrotalcite-derived Ni–Mg–Al mixed oxides: The influence of Ni content on catalytic activity, selectivity and stability. *Catal. Sci. Technol.* **2016**, *6*, 6705–6715. [[CrossRef](#)]
111. Debek, R.; Radlik, M.; Motak, M.; Galvez, M.E.; Turek, W.; Costa, P.D.; Grzybek, T. Ni-containing Ce-promoted hydrotalcite derived materials as catalysts for methane reforming with carbon dioxide at low temperature—on the effect of basicity. *Catal. Today* **2015**, *257*, 59–65. [[CrossRef](#)]
112. Debek, R.; Galvez, M.E.; Launay, F.; Motak, M.; Grzybek, T.; Costa, P.D. Low temperature dry methane reforming over Ce, Zr and CeZr promoted Ni–Mg–Al hydrotalcite-derived catalysts. *Int. J. Hydrogen Energy* **2016**, *41*, 11616–11623. [[CrossRef](#)]
113. Debek, R.; Motak, M.; Galvez, M.E.; Grzybek, T.; Costa, P.D. Influence of Ce/Zr molar ratio on catalytic performance of hydrotalcite-derived catalysts at low temperature CO₂ methane reforming. *Int. J. Hydrogen Energy* **2017**, *42*, 23556–23567. [[CrossRef](#)]
114. Düdler, H.; Kähler, K.; Krause, B.; Mette, K.; Köhl, S.; Behrens, M.; Scherer, V.; Muhler, M. Correction: The role of carbonaceous deposits in the activity and stability of Ni-based catalysts applied in the dry reforming of methane. *Catal. Sci. Technol.* **2014**, *4*, 3317–3328. [[CrossRef](#)]

115. Bae, J.W.; Kim, A.R.; Baek, S.C.; Jun, K.W. The role of CeO–ZrO distribution on the Ni/MgAlO catalyst during the combined steam and Co reforming of methane. *React. Kinet. Mech. Catal.* **2011**, *104*, 377–388. [[CrossRef](#)]
116. Baek, S.C.; Bae, J.W.; Cheon, J.Y.; Jun, K.W.; Lee, K.Y. Combined steam and carbon dioxide reforming of methane on Ni/MgAl₂O₄: Effect of CeO₂ promoter to catalytic performance. *Catal. Lett.* **2011**, *141*, 224–234. [[CrossRef](#)]
117. Christensen, K.O.; Chen, D.; Lødeng, R.; Holmen, A. Effect of supports and Ni crystal size on carbon formation and sintering during steam methane reforming. *Appl. Catal. A Gen.* **2006**, *314*, 9–22. [[CrossRef](#)]
118. Comas, J.; Dieuzeide, M.L.; Baronetti, G.; Laborde, M.; Amadeo, N. Methane steam reforming and ethanol steam reforming using a Ni(ii)-Al(iii) catalyst prepared from lamellar double hydroxides. *Chem. Eng. J.* **2006**, *118*, 11–15. [[CrossRef](#)]
119. Ochoa-Fernández, E.; Lacalle-Vilà, C.; Christensen, K.O.; Walmsley, J.C.; Rønning, M.; Holmen, A.; Chen, D. Ni catalysts for sorption enhanced steam methane reforming. *Top. Catal.* **2007**, *45*, 3–8. [[CrossRef](#)]
120. Dehghan-Niri, R.; Walmsley, J.C.; Holmen, A.; Midgley, P.A.; Rytter, E.; Dam, A.H.; Hungria, A.B.; Hernandez-Garrido, J.C.; Chen, D. Nanoconfinement of ni clusters towards a high sintering resistance of steam methane reforming catalysts. *Catal. Sci. Technol.* **2012**, *2*, 2476–2484. [[CrossRef](#)]
121. Takehira, K.; Shishido, T.; Wang, P.; Kosaka, T.; Takaki, K. Steam reforming of CH₄ over supported Ni catalysts prepared from a Mg–Al hydrotalcite-like anionic clay. *Phys. Chem. Chem. Phys.* **2003**, *5*, 3801–3810. [[CrossRef](#)]
122. Basile, F.; Benito, P.; Del, G.P.; Fornasari, G.; Gary, D.; Rosetti, V.; Scavetta, E.; Tonelli, D.; Vaccari, A. Highly conductive Ni steam reforming catalysts prepared by electrodeposition. *Chem. Commun.* **2008**, *0*, 2917–2919. [[CrossRef](#)] [[PubMed](#)]
123. Takehira, K.; Kawabata, T.; Shishido, T.; Murakami, K.; Ohi, T.; Shoro, D.; Honda, M.; Takaki, K. Mechanism of reconstitution of hydrotalcite leading to eggshelltype Ni loading on Mg–Al mixed oxide. *J. Catal.* **2005**, *231*, 92–104. [[CrossRef](#)]
124. Takeguchi, T.; Watanabe, H.; Murayama, T.; Takahashi, H.; Ueda, W. Quantitative analysis of coke formation during steam reforming of methane on a nickel–hydrotalcite catalyst under practical operation conditions. *Chem. Lett.* **2013**, *42*, 124–126. [[CrossRef](#)]
125. Takahashi, H.; Takeguchi, T.; Yamamoto, N.; Matsuda, M.; Kobayashi, E.; Ueda, W. Effect of interaction between Ni and YSZ on coke deposition during steam reforming of methane on Ni/YSZ anode catalysts for an Ir-sofc. *J. Mol. Catal. A Chem.* **2011**, *350*, 69–74. [[CrossRef](#)]
126. Homsí, D.; Aouad, S.; Gennequin, C.; Aboukais, A.; Abi-Aad, E. Hydrogen production by methane steam reforming over ru and cu supported on hydrotalcite precursors. *Adv. Mater. Res.* **2011**, *324*, 453–456. [[CrossRef](#)]
127. Lucrédio, A.F.; Assaf, E.M. Cobalt catalysts prepared from hydrotalcite precursors and tested in methane steam reforming. *J. Power Source* **2006**, *159*, 667–672. [[CrossRef](#)]
128. Natesakhawat, S.; Watson, R.B.; Wang, X.; Ozkan, U.S. Deactivation characteristics of lanthanide-promoted sol–gel Ni/Al₂O₃ catalysts in propane steam reforming. *J. Catal.* **2005**, *234*, 496–508. [[CrossRef](#)]
129. Ohi, T.; Miyata, T.; Li, D.; Shishido, T.; Kawabata, T.; Sano, T.; Takehira, K. Sustainability of Ni loaded Mg–Al mixed oxide catalyst in daily startup and shutdown operations of CH₄ steam reforming. *Appl. Catal. A Gen.* **2006**, *308*, 194–203. [[CrossRef](#)]
130. Takehira, K.; Ohi, T.; Miyata, T.; Shiraga, M.; Sano, T. Steam reforming of CH₄ over Ni–Ru catalysts supported on Mg–Al mixed oxide. *Top. Catal.* **2007**, *42–43*, 471–474. [[CrossRef](#)]
131. Miyata, T.; Li, D.; Shiraga, M.; Shishido, T.; Oumi, Y.; Sano, T.; Takehira, K. Promoting effect of Rh, Pd and Pt noble metals to the Ni/Mg(Al)O catalysts for the DSS-like operation in CH₄ steam reforming. *Appl. Catal. A Gen.* **2006**, *310*, 97–104. [[CrossRef](#)]
132. Miyata, T.; Shiraga, M.; Li, D.; Atake, I.; Shishido, T.; Oumi, Y.; Sano, T.; Takehira, K. Promoting effect of Ru on Ni/Mg(Al)O catalysts in DSS-like operation of CH₄ steam reforming. *Catal. Commun.* **2007**, *8*, 447–451. [[CrossRef](#)]
133. Li, D.; Zhan, Y.; Nishida, K.; Oumi, Y.; Sano, T.; Shishido, T.; Takehira, K. “Green” preparation of “intelligent” pt-doped Ni/Mg(Al)O catalysts for daily start-up and shut-down CH₄ steam reforming. *Appl. Catal. A Gen.* **2009**, *363*, 169–179. [[CrossRef](#)]
134. Takehira, K. Highly dispersed and stable supported metal catalysts prepared by solid phase crystallization method. *Catal. Surv. Asia* **2002**, *6*, 19–32. [[CrossRef](#)]

135. Basile, F.; Basini, L.; Fornasari, G.; Gazzano, M.; Trifiro, F.; Vaccari, A. Cheminform abstract: New hydrotalcite-type anionic clays containing noble metals. *Chem. Commun.* **1996**, *21*, 2435–2436. [[CrossRef](#)]
136. Basile, F.; Basini, L.; Amore, M.D.; Fornasari, G.; Guarinoni, A.; Matteuzzi, D.; Piero, G.D.; Trifirò, F.; Vaccari, A. Ni/Mg/Al anionic clay derived catalysts for the catalytic partial oxidation of methane: Residence time dependence of the reactivity features. *J. Catal.* **1998**, *173*, 247–256. [[CrossRef](#)]
137. Basile, F.; Fornasari, G.; Trifirò, F.; Vaccari, A. Rh–Ni synergy in the catalytic partial oxidation of methane: Surface phenomena and catalyst stability. *Catal. Today* **2002**, *77*, 215–223. [[CrossRef](#)]
138. Basile, F.; Benito, P.; Fornasari, G.; Monti, M.; Scavetta, E.; Tonelli, D.; Vaccari, A. Novel rh-based structured catalysts for the catalytic partial oxidation of methane. *Catal. Today* **2010**, *157*, 183–190. [[CrossRef](#)]
139. Ballarini, A.; Benito, P.; Fornasari, G.; Scelza, O.; Vaccari, A. Role of the composition and preparation method in the activity of hydrotalcite-derived Ru catalysts in the catalytic partial oxidation of methane. *Int. J. Hydrogen Energy* **2013**, *38*, 15128–15139. [[CrossRef](#)]
140. Velasco, J.A.; Fernandez, C.; Lopez, L.; Cabrera, S.; Boutonnet, M.; Järås, S. Catalytic partial oxidation of methane over nickel and ruthenium based catalysts under low O₂/CH₄ ratios and with addition of steam. *Fuel* **2015**, *153*, 192–201. [[CrossRef](#)]
141. Harada, M.; Domen, K.; Hara, M.; Tatsumi, T. Ba-Co-Fe-Nb-O dense ceramic as an oxygen permeable membrane for partial oxidation of methane to synthesis gas. *Chem. Lett.* **2006**, *35*, 1326–1327. [[CrossRef](#)]
142. Lucrédio, A.F.; Jerkiewicz, G.; Assaf, E.M. Cobalt catalysts promoted with cerium and lanthanum applied to partial oxidation of methane reactions. *Appl. Catal. B Environ.* **2008**, *84*, 106–111. [[CrossRef](#)]
143. Choudhary, V.R.; Mamman, A.S. simultaneous oxidative conversion and CO₂ or steam reforming of methane to syngas over CoO–NiO–MgO catalyst. *Fuel Energy Abstr.* **2000**, *73*, 345–350. [[CrossRef](#)]
144. Luneau, M.; Schuurman, Y.; Meunier, F.C.; Mirodatos, C.; Guilhaume, N. High-throughput assessment of catalyst stability during autothermal reforming of model biogas. *Catal. Sci. Technol.* **2015**, *5*, 4390–4397. [[CrossRef](#)]
145. Souza, M.M.V.M.; Ribeiro, N.F.P.; Neto, O.R.M.; Cruz, I.O.; Schmal, M. Autothermal reforming of methane over nickel catalysts prepared from hydrotalcite-like compounds. *Stud. Surf. Sci. Catal.* **2007**, *167*, 451–456.
146. Takehira, K.; Shishido, T.; Wang, P.; Kosaka, T.; Takaki, K. Autothermal reforming of CH₄ over supported Ni catalysts prepared from Mg–Al hydrotalcite-like anionic clay. *J. Catal.* **2004**, *221*, 43–54. [[CrossRef](#)]
147. Halabi, M.H.; Croon, M.H.J.M.D.; Schaaf, J.V.D.; Cobden, P.D.; Schouten, J.C. Reactor modeling of sorption-enhanced autothermal reforming of methane. Part I: Performance study of hydrotalcite and lithium zirconate-based processes. *Chem. Eng. J.* **2011**, *168*, 872–882. [[CrossRef](#)]
148. Halabi, M.H.; Croon, M.H.J.M.D.; Schaaf, J.V.D.; Cobden, P.D.; Schouten, J.C. Reactor modeling of sorption-enhanced autothermal reforming of methane. Part II: Effect of operational parameters. *Chem. Eng. J.* **2011**, *168*, 883–888. [[CrossRef](#)]

